II

INTRODUCTION. BOUNDARY LAYER THEORY

1. Vorticity and the development of fluid flows

1.1. *Introduction*

THE object of this chapter is to describe qualitatively the position and significance of boundary layers in fluid flows, as a background to the more detailed and quantitative information given in later chapters.

Prandtl (1904) introduced the boundary-layer theory in the first instance to resolve, for flows in which the Reynolds number is large (which were shown in Section I. 5.3 to include most flows of practical importance), the difficulty referred to in Section I. 1 and at the end of Section I. 5.5—namely, that the 'irrotational' or 'potential' flow solutions derived by neglecting viscosity (that is, putting $R = \infty$) do not satisfy the boundary condition at a solid surface. Rather, they require slip over the surface, which we have seen is impossible.

Prandtl's suggestion was that one might resuscitate such irrotational flows by postulating the existence, between them and the solid surface, of a thin layer of fluid in which the velocity increased steeply from zero at the wall to the theoretical surface value at the edge of the layer. In such a 'boundary layer', where the velocity gradient is high, viscosity would be important (or else, indeed, the layer would appear already in the inviscid theory). Prandtl now asked the question: does the mechanics of such a layer, when viscous effects are included, permit a development in which it remains thin all along the surface? Clearly, if it does, then the irrotational-flow approximation will have considerable value, and the drag coefficient will be small—that is, close to the value 0 given by that approximation. This is the case, as we shall see, for many obstacles, of the kind usually described as 'streamlined'. If, alternatively, the mechanics of the layer indicates development up to a catastrophe, in which fluid retarded by viscous forces breaks right away from the surface, disturbing large areas of the flow field, then clearly the original irrotational flow ceases to have value as an approximation, and new considerations become necessary. The flow is described in this case as 'separated'.

Experimental work has supported the correctness of Prandtl's assumptions; methods to be described in Chapter X have shown, not only that the boundary layer exists, but also that the velocity distribution across it develops in accordance with the mechanics to be discussed below. They showed, too, under what conditions the steady 'laminar' boundary layer develops instabilities and becomes 'turbulent' (Section 3), and Prandtl (1914, 1927) was again the discoverer of the effects of this transition on the mechanics of the layer—notably, in delaying separation—and on the variation with Reynolds number (Section 4) of the flow patterns around bluff and streamlined bodies.

Now, the desired mechanics of a boundary layer can be very effectively discussed in terms of momentum changes due to convection, viscous diffusion, and the action of pressure gradients. A qualitative view of this theoretical approach, which throws valuable light on the behaviour of a wide variety of particular flows, is given in Section 2.9. On the other hand, both to explain convincingly the existence of boundary layers, and, also, to show what consequences of flow separation (including matters of such practical importance as the effect of trailing-vortex wakes) may be expected, arguments concerning vorticity are needed. In addition, these alone explain (as in the classical inviscid theory) why the flow outside the boundary layer and wake should be irrotational.

We see, then, that, although momentum considerations suffice to explain the local behaviour in a boundary layer, vorticity considerations are needed to place the boundary layer correctly in the flow as a whole. It will also be shown (surprisingly, perhaps) that they illuminate the detailed development of the boundary layer (see Sections 2.1–2.8) just as clearly as do momentum considerations (which are briefly described in Section 2.9).

Accordingly, this Section 1 is concerned mainly with vorticity and with its relation to the development of fluid flows, in preparation for the discussion of boundary-layer mechanics in Section 2. A simplified treatment is used, to avoid the sometimes forbidding aspect of vorticity theory. (One can of course regard some of these simple arguments as being fully justified only by the more mathematical deductions of Chapter III; see also Lamb 1932, Truesdell 1954.)

1.2. *Vorticity*

The vorticity at any point in a fluid flow is proportional to the instantaneous angular momentum of a spherical particle of fluid centred

on the point. One can regard the motion of such a small sphere of fluid as a combination (Fig. II. 1) of three motions:

(i) Uniform translation with the velocity **v** of the centre. All the momentum of the sphere's motion is in this part.

(ii) Rotation, with the angular velocity and the direction of the axis of rotation specified by the vector $\frac{1}{2}\boldsymbol{\omega}$, where $\boldsymbol{\omega} = \operatorname{curl}\mathbf{v}$ is the vorticity. All the angular momentum of the sphere's motion is in this part.

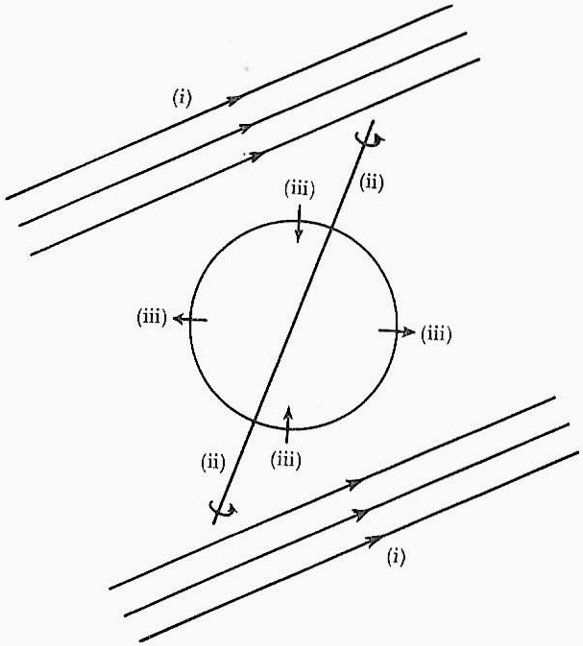

FIG. II. 1. Resolution of the motion of a small fluid sphere into (i) translation, (ii) rotation, (iii) straining.

(iii) A symmetrical squeezing, or 'straining', which is changing the sphere into an ellipsoid (thus elongating it in some directions and foreshortening it in others). This motion has no net linear or angular momentum.

Note that the motion of a *rigid* sphere is composed simply of (i) and (ii), a translation and a rotation. *Fluid* spheres, however, are in general always changing shape. For a small sphere, the instantaneous rate of change of shape consists always of a uniform elongation process in one direction, a uniform foreshortening process in a second direction, at right angles to the first, and a third process (which may be either elongation or foreshortening) in a third direction at right angles to the

first two. These three directions are the axes of the ellipsoid mentioned under heading (iii), and are usually called the 'principal axes of rate-of-strain' of the fluid particle.

If these axes were taken as the coordinate axes, then the rates of elongation in the three directions would be $\partial v_x/\partial x$, $\partial v_y/\partial y$, $\partial v_z/\partial z$. It is of course the solenoidality condition (Section I. 2.5) that ensures, because their sum is zero, that if one of these is positive then at least one other must be negative (indicating a foreshortening), and vice versa.

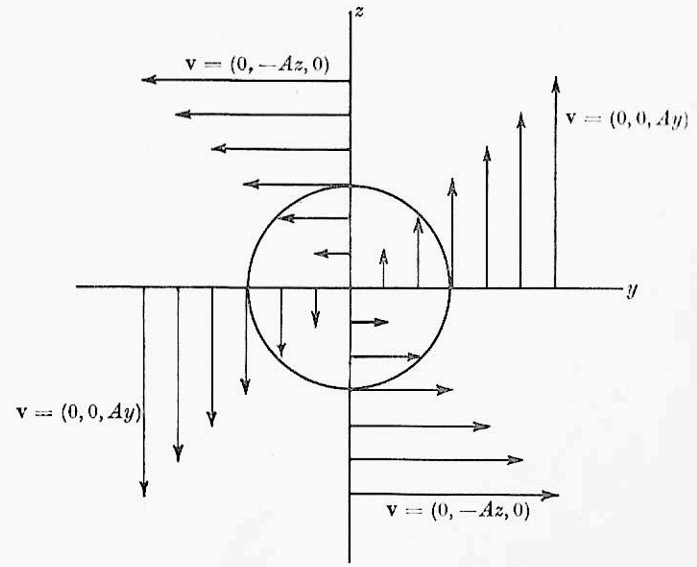

FIG. II. 2. Because the vector sum of the two shear flows shown is a uniform rotation with angular velocity A, in which the angular momentum of the sphere is IA, the angular momentum in one shear flow alone (for example, that with $\partial v_z/\partial y = A$) is $\frac{1}{2}IA$.

The expressions for the components of the vorticity,

$$\boldsymbol{\omega} = \operatorname{curl}\mathbf{v} = \left(\frac{\partial v_z}{\partial y} - \frac{\partial v_y}{\partial z}, \frac{\partial v_x}{\partial z} - \frac{\partial v_z}{\partial x}, \frac{\partial v_y}{\partial x} - \frac{\partial v_x}{\partial y}\right), \tag{1}$$

are easily understood from Fig. II. 2, which shows, for example, that the shear term $\partial v_z/\partial y$ produces an angular momentum $\frac{1}{2}I\,\partial v_z/\partial y$ about the x-axis, where I is the sphere's moment of inertia. The signs of the terms in (1) reflect that a rotation about (say) the x-axis is called positive (in a right-handed system of axes) if it is in the direction of turning of a right-handed screw moving along the positive x-axis, and negative if it is in the opposite direction.

Expressions (1) imply that $\boldsymbol{\omega}$, like $\mathbf{v}$, satisfies the solenoidality condition

$$\operatorname{div}\boldsymbol{\omega} = \frac{\partial\omega_x}{\partial x}+\frac{\partial\omega_y}{\partial y}+\frac{\partial\omega_z}{\partial z} = 0. \tag{2}$$

Geometrically, this means (Section I. 2.5) that the magnitude of the vorticity varies along any 'elementary vortex tube' (thin tube to which

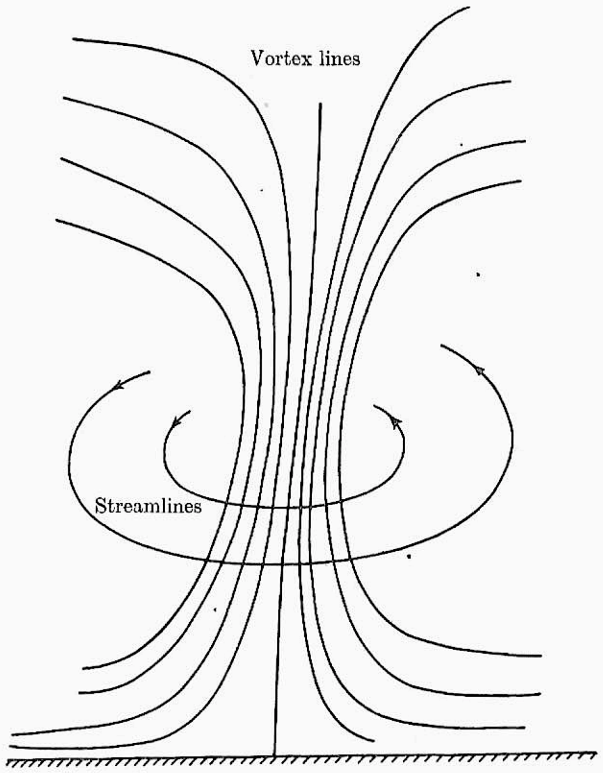

FIG. II. 3. Vortex lines in a whirlwind.

the *vorticity* vector is everywhere tangential) inversely as the cross-sectional area. To represent a vorticity field pictorially, one may imagine it honeycombed with such vortex tubes, each of the same 'strength' (product of cross-sectional area and vorticity magnitude)—the position of each tube being indicated by a 'vortex line' (*curve* to which the vorticity vector is everywhere tangential) threaded centrally down it. Wherever these vortex lines congregate densely, the associated tubes have reduced cross-sectional area and the vorticity is correspondingly great.

Such vortex lines cannot end abruptly in the fluid, whence it is sometimes stated that they either form closed 'vortex loops' *or* end on a solid surface. It is worth noting, however, that the no-slip condition makes the latter alternative impossible (except for isolated vortex lines, similar to 'dividing streamlines' in velocity fields) at any solid surface at rest (or in pure translational motion), where necessarily the normal component of vorticity is zero. Hence, in flows which do not contain rotating bodies, *all* vorticity appears in closed loops. It is usually instructive, in flows where the vortex lines appear to be predominantly in one direction, to consider where they in fact turn round to form closed loops—those in a whirlwind, for example, turning in the boundary layer on the ground and proceeding nearly horizontally until they reach anticyclonic regions where they can rise and join the vortex lines high in the atmosphere which have been making a similar horizontal progress above the region of high wind (Fig. II. 3).

1.3. *Variation of vorticity in an inviscid fluid*

Consider next how the vorticity varies with time, in the first place with viscosity neglected. In this case, the rate of change of angular momentum of the fluid sphere of Section 1.2 must be zero, since the pressure forces at its boundary all act through the centre, and so does the force of gravity (and, indeed, it may be shown more generally that the resultant over a homogeneous sphere of any conservative field of external forces acts through its centre).

This vanishing of the rate of change of angular momentum does not imply conservation of the angular velocity $\frac{1}{2}\boldsymbol{\omega}$ of part (ii) of the sphere's motion, since part (iii) in general is altering its moments of inertia. It means rather that, as the sphere becomes ellipsoidal, the *component* of angular velocity about each of the principal axes of rate-of-strain is changing in *inverse* proportion to the moment of inertia about that axis—which implies variation in *direct* proportion to the length of that axis. Thus, vorticity components about axes that are being elongated are increasing (just as any spinning body spins faster if its girth is reduced by stretching of the axis of rotation); while those about axes that are being foreshortened are decreasing.

To represent this result pictorially (Fig. II. 4), one may draw an arrow in the direction of the vorticity vector $\boldsymbol{\omega}$, and proportional to it in length, both for the initial spherical state of the particle and also an instant later (when it has become ellipsoidal). The results, that the elongation of $A'OA$ is increasing the component of $\boldsymbol{\omega}$ in this direction,

in proportion to the increased length of that axis, while the foreshortening of $B'OB$ decreases the component of $\boldsymbol{\omega}$ in that direction in proportion to the length $B'OB$, with a third similar result in the $C'OC$ direction (not shown on the figure), mean that the variation of $\boldsymbol{\omega}$ can be obtained by applying these elongations and foreshortenings directly to the arrow itself.

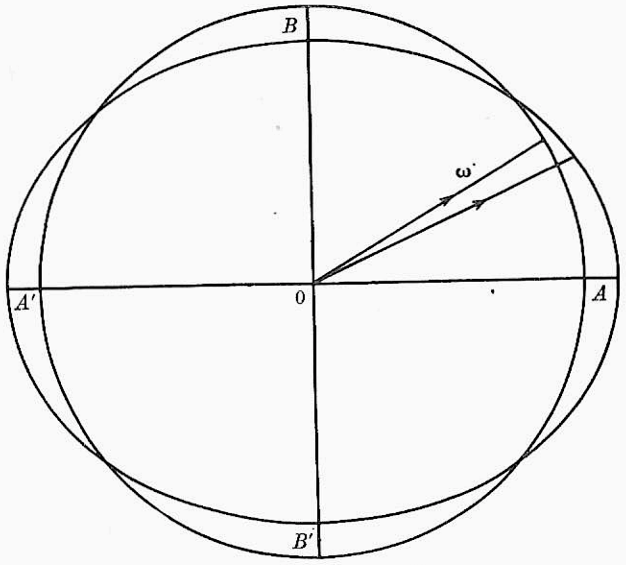

FIG. II. 4. Variation of the vorticity of a fluid particle due to straining.

In other words, the arrow may be thought of as a little arrow-shaped element of fluid—subject, like the whole spherical particle, to precisely these elongations and foreshortenings. The variation of vorticity with time is exhibited both in magnitude and direction by the changes in length, direction and position of this arrow-shaped element. The changes in *position* arise from convection by the translational component (i) of the motion of one small fluid sphere; these are essential to the accuracy of representation, since of course the changes of angular momentum and vorticity discussed above were changes for the particle as it moved about, and not changes at a fixed point of space. The arrow-shaped element would, on the other hand, be unmoved by the rotational component (ii), on whose axis it lies. (It appears paradoxical that the arrow is turned round only by the part (iii) of the motion which is 'without rotation'; but it must be remembered that only the total angular momentum of the sphere is zero for this part of the motion, and not that of individual asymmetrically shaped bits.)

To sum up: if one imagines a fluid flow at any instant as including millions of tiny arrow-shaped elements of fluid, each pointing in the direction of the local vorticity, and of length proportional to its magnitude, then, if viscosity can be neglected, these individual arrow-shaped elements will move so that at all subsequent times they give the same information with equal accuracy.

This is the result stated by Helmholtz in the form 'vortex lines move with the fluid'. Vortex lines, obtained by suitably joining up the arrows, are curves (Section 1.2) to which the vorticity vector is everywhere tangential. Helmholtz's statement by itself shows only how the direction of $\boldsymbol{\omega}$ changes, but if one adds that the magnitude varies in proportion as the vortex line is locally *stretched*, the combined statement becomes equivalent to that just given.

A particular case of the result is Lagrange's theorem, that fluid which at one instant has vanishing vorticity will also have vanishing vorticity at later instants, if viscosity can be neglected. For the fluid motion cannot stretch any arrow by an *infinite* factor, as clearly would be necessary to convert zero vorticity into non-zero vorticity.

1.4. *Variation of vorticity in a viscous fluid*

In a real fluid, the angular momentum of the sphere discussed in Section 1.3 changes, as a result of tangential stresses proportional to the viscosity. This leads to an additional term in the rate of change of vorticity, which can be interpreted as due to diffusion with diffusivity ν. For each term in the expression (1) for $\boldsymbol{\omega}$ is proportional to a momentum gradient, whose change due to viscosity must correspond to diffusion with this diffusivity, simply because this is so for the momentum itself (Section I. 3.4).

The inertial rate of change of $\boldsymbol{\omega}$ for a fluid particle, represented by the turning and stretching of the vortex lines, must accordingly be supplemented by a diffusion term $\nu\nabla^2\boldsymbol{\omega}$. The corresponding contribution of diffusion to the rate of change of the 'total vorticity' in any volume of fluid (integral of vorticity over it) is equivalent to a flow, across unit area of its surface, at a rate ν times the gradient of $\boldsymbol{\omega}$ along the outward normal.

This important idea of vorticity flow across a surface (so closely parallel to that of heat flow) cannot be viewed as diffusion of angular momentum; vorticity is proportional to the angular momentum of a spherical particle about its mass centre, and when it diffuses from one particle to another the relevant angular momentum is about quite a

different point. The correct view relates diffusion of vorticity to that of momentum, through that of momentum gradient, as indicated above.

1.5. *Solid boundaries as sources of vorticity*

The last conclusion of Section 1.3, that a particle of fluid with zero vorticity will continue to have zero vorticity, is false in a viscous fluid, since diffusion of vorticity from nearby particles can occur. But diffusion cannot create vorticity out of nothing, so that in external aerodynamics one may reasonably ask: when a uniform stream flows past an obstacle, how is vorticity imparted to the fluid, all of which lacks it initially?

The answer is that the solid boundary is a *distributed source* of vorticity (just as, in some flows, it may be a distributed source of heat). To convince oneself of this, it suffices to examine any of the known exact solutions of the equations of motion (Chapter III), and to observe that at almost all points of the boundary the vorticity has a non-zero gradient along the normal. This gradient, multiplied by $(-\nu)$, represents (Section 1.4) the flow of 'total vorticity' out of the solid surface per unit area per unit time, so that it is the local *strength* of the surface distribution of vorticity sources. A physical explanation of the need for vorticity creation at the boundary is postponed to Section 1.7.

The tangential-vorticity source strength has a simple relation to pressure gradient, at least for flow over a stationary plane surface. If the surface is taken as $z = 0$, the flow of x-vorticity out of it is

$$-\nu \frac{\partial \omega_x}{\partial z} = -\nu \frac{\partial}{\partial z}\left(\frac{\partial v_z}{\partial y} - \frac{\partial v_y}{\partial z}\right) = \nu \frac{\partial^2 v_y}{\partial z^2} = \nu \nabla^2 v_y = \frac{1}{\rho}\frac{\partial p}{\partial y}, \tag{3}$$

since v_x, v_y, v_z are zero on $z = 0$ (whence all their derivatives with respect to x and y vanish, and hence also $\partial v_z/\partial z = 0$ by the solenoidality condition), and because at a solid surface transfer of momentum by convection is absent, so that transfer by diffusion must exactly balance transfer by pressure gradient.

It follows from (3) that the tangential vorticity created is in the direction of the surface isobars (the sense of rotation being that of a ball rolling down the line of steepest pressure fall), and that the source strength per unit area is of magnitude ρ^{-1} times the pressure gradient. (To see this, take the x-direction first tangent, and then normal, to an isobar.) It is significant that this expression does not vanish if the viscosity is made to tend to zero. On curved surfaces the corresponding result is not exact, but, for high Reynolds number, we shall find that it is still a good approximation. Also, normal-vorticity production is then an effect of smaller order. It is required, in general, to maintain

the solenoidality condition (2) on $\boldsymbol{\omega}$, which, indeed, relates the normal-vorticity source strength directly to the surface distribution of tangential vorticity, by the equation

$$-\nu \frac{\partial \omega_z}{\partial z} = +\nu\left(\frac{\partial \omega_x}{\partial x} + \frac{\partial \omega_y}{\partial y}\right). \tag{4}$$

In the next two sections it will be seen how the vorticity which is produced at the surface, and carried away from it by diffusion and convection, determines the entire flow, whose development in turn controls the production of vorticity.

1.6. *The vorticity distribution as fixing the flow field*

A special case of the unique determination of the flow field by the vorticity distribution is the theorem of classical hydrodynamics (Lamb 1932, chapter iii) that, if a body moves through unlimited fluid which far from the body is at rest (which, as observed in Section 1.1, produces motions equivalent to those of external aerodynamics), then one and only one flow, with *zero* vorticity everywhere, satisfies the boundary condition of zero *normal* relative velocity at the solid surface—supposed 'without holes' or, more precisely, such that the region outside it is simply connected. Such an 'irrotational' motion in such a region has necessarily a 'velocity potential' ϕ, with

$$\mathbf{v} = \operatorname{grad}\phi; \quad \text{that is,} \quad v_x = \partial\phi/\partial x,\ v_y = \partial\phi/\partial y,\ v_z = \partial\phi/\partial z. \tag{5}$$

The solenoidality condition on $\mathbf{v}$ becomes Laplace's equation,

$$\nabla^2\phi = 0; \quad \text{that is,} \quad \partial^2\phi/\partial x^2 + \partial^2\phi/\partial y^2 + \partial^2\phi/\partial z^2 = 0. \tag{6}$$

The theorem stated then follows from the fact (Kellogg 1929, chapter xi) that (6), together with the condition $\operatorname{grad}\phi \to 0$ at infinity, and the boundary condition

$$\partial\phi/\partial n = v_{wn} \tag{7}$$

(where the gradient of ϕ along the normal to the surface, $\partial\phi/\partial n$, is the normal component of the fluid velocity, and v_{wn} is the normal velocity component of the solid surface itself), fix ϕ uniquely, except to within an arbitrary constant whose value does not affect the velocity components (5).

A particular case of the theorem says that, at any instant when the body is *not* moving, the fluid must be at rest (if the other assumptions, notably irrotationality, are satisfied). Indeed, one proves this first (by applying the 'divergence theorem' to the vector $\phi\mathbf{v}$), and infers that two solutions of the more general problem are necessarily identical, because by (7) their difference must satisfy $\partial\phi/\partial n = 0$, which is the condition at a stationary surface.

In this chapter we need the still more general result (Lamb 1932, chapter vii) that, for *any* given solenoidal distribution of vorticity $\boldsymbol{\omega}$ outside the body surface (whose motion is again prescribed), one and only one solenoidal velocity field exists, tending to zero at infinity and with zero normal relative velocity at the solid surface. The proof of this result is in two parts. First, we write down a velocity field $\mathbf{v}_0$ which has the given vorticity distribution and tends to zero at infinity. This is given by the Biot–Savart law,

$$\mathbf{v}_0 = \int \frac{\boldsymbol{\omega}\times\mathbf{r}}{4\pi r^3}\, dV, \tag{8}$$

where the integration is over the whole vorticity field and $\mathbf{r}$ is the position vector relative to the volume element dV. The relationship (8) is the same as for the magnetic field $\mathbf{H}$ produced by a steady current distribution of density $\mathbf{i}$ (which in rationalized electromagnetic units equals curl $\mathbf{H}$). It means that the vorticity $\boldsymbol{\omega}$ in each volume element dV induces a rotation of all the fluid at a distance r from it with angular velocity $\boldsymbol{\omega}\, dV/4\pi r^3$.

In general, $\mathbf{v}_0$ does not satisfy the boundary condition for $\mathbf{v}$. However, the difference $\mathbf{v}-\mathbf{v}_0$ must be irrotational (since curl $\mathbf{v}_0 = \boldsymbol{\omega}$), and hence equal to grad ϕ for some potential ϕ. On the body surface,

$$\frac{\partial\phi}{\partial n} = v_n - v_{0n} = v_{wn} - v_{0n}, \tag{9}$$

which is fixed, and also grad $\phi \to 0$ at infinity. As we have seen, just one ϕ (except for an arbitrary additive constant) satisfies these conditions.

This addition grad ϕ to the Biot–Savart velocity field is sometimes described as the field of the image vorticity, since for simple shapes of boundary (planes, circular cylinders, spheres) it can be easily related by the same Biot–Savart formula to a distribution of 'virtual' or 'image' vorticity within the body (Lighthill 1956*b*).

Two notable features of these theorems are the instantaneous response of the flow to changes in the body's movements, and the unique determination of even a rotational flow by the boundary condition on the normal velocity component alone. The first feature is not paradoxical, because of the effective assumption of infinite velocity of the sound waves with which irrotational disturbances are propagated, which is implied by the conditions (I. 9) for solenoidality; the second will be fully discussed in Section 1.7. We note also Kelvin's result (Lamb 1932, p. 47), that the kinetic energy of one of these motions with vorticity is necessarily greater than that of the irrotational flow satisfying the same boundary conditions, by an amount equal to the kinetic energy of the flow which would be induced by the vorticity with the boundary at rest. This means that it is the irrotational flow which least disturbs the fluid through which the body moves.

1.7. *Flow development*

We now ask the question: how does a body moving through otherwise undisturbed fluid determine the development of the flow around it? The answer may be considered given if we can describe how a computing machine of sufficiently large capacity could calculate to sufficient accuracy how the flow field changes, progressing by suitably small steps forward in time.

Until recently, such an account would have been of largely theoretical value, as showing how the conditions (including boundary conditions) derived in Chapter I determine uniquely the flows under discussion. (This is not obvious, particularly since there is no information on the variation of pressure, except that the effect of pressure-gradient forces on the velocity field must constantly be such as to keep it solenoidal.) However, the development of digital computers of really high speed and capacious memory has given practical value to such considerations; already two important cases of flow development have been computed by the method described below (Payne 1956, 1958), and much further work is planned, while closely analogous methods are being used in numerical weather forecasting. Alternative methods, attaching cardinal importance to the pressure or a stream function in place of vorticity, are inadequate both theoretically and practically, for reasons to be mentioned at the end of this section.

The results of Section 1.6 show that it is sufficient to study the development of the vorticity field around the body, because for a given movement of the body this determines the whole flow—and, indeed, 'over-determines' it, requiring only the boundary condition on the normal velocity component at the surface to fix the flow uniquely. Thus, there is only a restricted class of vorticity distributions that correspond to real flows satisfying also the no-slip condition on the tangential velocity.

For a step-by-step computation of vorticity development, we need a method of progressing from one vorticity distribution within this restricted class to the vorticity distribution a short time later. The results of Sections 1.3 and 1.4 show how this is to be achieved away from the body surface. The rate of change of vorticity is that generated by the flow field in convecting and stretching the vortex lines, as

discussed in Section 1.3, plus that produced by viscous diffusion (Section 1.4). To complete our knowledge of the vorticity field at the later instant, we must determine the rate of production of vorticity at the boundary.

Relations between tangential-vorticity source strength and pressure gradient (Section 1.5) are *not* useful here, since the pressure has been eliminated from the problem (rightly, as a variable whose rate of change is unknown) by our concentration on vorticity. Equally, the expression for vorticity source strength $-\nu\,\partial\boldsymbol{\omega}/\partial z$ (where z = normal distance from boundary) is valueless, for diffusion (which, of course, dominates over convection near to the boundary) tends to spread the vorticity created at any instant $t = \tau$ according to a Gaussian distribution

$$e^{-z^2/4\nu(t-\tau)}\{\pi\nu(t-\tau)\}^{-\frac{1}{2}}, \tag{10}$$

so that the contribution to the expression $-\nu\,\partial\boldsymbol{\omega}/\partial z$ at time t from a source at any previous instant is zero, although the integrated effect up to time t may be shown to be equal to the source strength at time t. This means that the instantaneous source strength *determines* the normal gradient and *not* vice versa. On the other hand, the normal-vorticity source strength is expressible directly in terms of *tangential* gradients of vorticity as in (4), which incidentally ensures that the vorticity field remains solenoidal. Accordingly, it is only the values of the tangential-vorticity source strengths that remain in doubt.

To find these, we first suppose them zero and proceed to the next stage of our problem—determining the velocity field at the later instant from the vorticity field. This, as shown in Section 1.6, requires only a knowledge of the normal velocity at the surface. The resulting tangential velocity at the surface may *not* satisfy the no-slip condition. In this case, we deduce that exactly enough tangential vorticity must have been created at the surface, during the time interval in question, so that the velocity field of that vorticity (which during such a short interval has diffused only a very small distance from the surface) combines with that previously determined to give zero slip.

For example, at a point where the slip-velocity component v_x (the x-direction being tangential to the wall) is calculated as X after the interval δt, we deduce that, during the interval, 'total' y-vorticity X per unit area has been generated. This forms a 'vortex sheet', corresponding to a velocity field falling, from zero beyond a distance which is small of order $\sqrt{(\nu\,\delta t)}$, to $-X$ at the surface. Its distribution, easily derived by simple diffusion theory, is not needed in practical calculations of vorticity and velocity at the mesh-points of a lattice, since the time interval δt is always taken so small that this additional velocity field affects significantly the velocity only at mesh-points on the surface (reducing the slip to zero); accordingly, the expression for the total tangential vorticity generated at the surface in time δt is all that is needed to proceed to the next instant.

To sum up: any flow development is in principle computable by studying the diffusion of vortex lines, and their convection and stretching by the associated flow, while supposing normal and tangential vorticity to appear at the surface continuously, in just such measure as is required to maintain, respectively, the solenoidality of the vorticity field and the no-slip condition. For practical details of the computation of particular unsteady flows by this method, see Payne (1956, 1958).

The method has many advantages over other approaches. Note that, even for 'two-dimensional' flows, the employment of a 'stream function' ψ gains nothing, since the equation (III. 38) which governs it gives the rate of change not of ψ but of $\nabla^2\psi$, which *is* the vorticity. Alternatively, the problem might be approached by determining at each stage what pressure field will maintain solenoidality of the velocity field everywhere; this involves solving an equation of Poisson's type for the pressure, before using the momentum equation to derive the velocity field at the next instant. In a practical problem this introduces the difficulty of operating in the whole infinite flow field, instead of in the region of non-zero vorticity, which includes only those portions of fluid that have passed near the body surface. A second difficulty is that the fluid velocities respond by large sudden changes to any sudden alteration in the velocity or angular velocity of the solid surface, while pressures have enormous peaks (the so-called 'impulsive pressures') during such changes; on the other hand, the vorticity distribution varies smoothly, and the method described above operates unaltered during such changes.

Advantages of thinking in terms of vorticity, the only flow quantity whose values are not propagated at the enormous speed of sound, become particularly clear from examples in Section 2, but we may conclude Section 1 by an even simpler example. When one blows out a candle some distance away, the airflow during the puff consists of an irrotational 'source' flow in addition to the vorticity-induced flow. However, such irrotational flows fall off rapidly with distance. Accordingly, the candle does not respond until later, when the lip-generated 'vortex

ring', each portion of which induces a forward motion in the others, has reached the candle. It would be hard to explain this motion by direct consideration of pressure-velocity interactions.

2. Boundary layers and separation

2.1. *The development of a laminar boundary layer*

In Section 2, the study of flow development, including development to a possible steady flow, is pursued, without any discussion of the stability of the motions under the small disturbances which are always present. Some (though not all) of the conclusions will have to be modified in the light of the evidence on flow instability and the effects of turbulence which is presented in Section 3. However, the latter material is understood more easily after a full discussion of the mechanics of 'laminar' flow, that is, of flow in which no such amplification of the effects of small disturbances is supposed to have occurred.

The boundary-layer concept can appropriately be introduced by discussing a flow started up from rest when a stationary body begins suddenly to move through fluid with uniform velocity U_∞. In our discussion of this flow, all velocities will be specified relative to the body, so that we think of the flow of a uniform stream past a body, starting instantaneously at time $t = 0$.

At this instant, no vorticity has been created, and hence the flow around the body is the irrotational one. Immediately, however, as Section 1.7 shows, this creates tangential vorticity at the boundary—concentrated in the form of a 'vortex sheet', which just permits the irrotationally flowing fluid to slip over the fluid at rest in contact with the boundary. All this vorticity then diffuses out from the boundary, in proportion to $(\pi\nu t)^{-\frac{1}{2}}\exp(-z^2/4\nu t)$ (see (10)), the speed of this diffusion in its very earliest stages being much greater than any convection speed, which can therefore be neglected in comparison. The body is then surrounded by a vortex layer 'of uniform thickness'. To speak thus of the 'thickness' of the layer is not absurd, since the exponential falls to zero extremely fast when z increases above about $3\sqrt{(\nu t)}$; but, to get a precise measure of thickness, one may, for example, consider the distance of vortex elements from the surface and evaluate their average δ_1 (which for reasons to appear will be called the 'displacement thickness' of the layer) as

$$\delta_1 \sim 2\sqrt{(\nu t/\pi)} \quad \text{for small } t. \tag{11}$$

In this early stage no normal vorticity is created; expression (4) may be shown to vanish owing to the irrotationality of the external flow.

Further, the influence of the vortex layer is felt almost entirely inside itself, producing a velocity variation across it, from the surface value zero to the non-zero 'surface' value predicted by irrotational-flow theory. Such change as does occur in the irrotational flow outside the vortex layer may be estimated by replacing the layer, to a first approximation, by a concentrated vortex sheet at the mean distance δ_1 of vorticity from the surface (Lighthill 1958). This replacement reduces to rest the flow inside the sheet, while the flow outside it is irrotational and slips freely over it; therefore, by the uniqueness theorem, the latter flow is that around a modified body, with surface displaced outwards into the fluid by the 'displacement thickness' δ_1. Thus, the vortex layer, when thin enough for this approximation to be good, alters the irrotational flow into one around a thickened body.

The simplicity of such a 'boundary layer' of vorticity dominated entirely by diffusion persists for only a very short time. As soon as the body has moved through even a small percentage of its length, convection begins to redistribute the vorticity which has been created. The vortex lines, which may be shown to lie initially along the surface equipotentials of the irrotational flow, are carried around the body, leading to a distribution of vorticity that no longer corresponds to zero slip at the surface. By Section 1.7 this requires the generation of new tangential vorticity, which may be in a quite different (or indeed opposite) direction from that originally created (see Section 2.8 below). This in turn is convected downstream, a redistribution which leads to still further vorticity production at the surface.

We may now ask: will these processes yield ultimately a steady-flow field, and, if so, how and of what kind? Even if the matter of stability be disregarded, we cannot yet give these questions their precise answers, whose immense complication (at least!) is embarrassingly clear from Chapters IV to VIII. However, some essential parts of the answers follow plainly from the above discussion.

2.2. *Boundary layers and wakes in steady flow*

First, it is possible for convection to prevent the 'boundary layer', that is, the region of vorticity near the surface, from growing beyond a thickness of order $\sqrt{(\nu l/U_\infty)}$, which is much smaller than the scale l of the body provided that $R = U_\infty l/\nu$ is large. For the vorticity in the outer parts of the boundary layer is convected downstream at a speed which is close to that of the irrotational flow outside the layer, and therefore of order U_∞; hence, the time since its generation remains at

most of order l/U_∞, during which it can have diffused a distance at most of order $\sqrt{(\nu l/U_\infty)}$ away from the surface. Here, it is assumed that *convection* has not greatly altered its distance from the surface, in other words, that the streamlines near the surface are closely parallel to it; this rule is generally correct, but has important exceptions which will shortly be discussed.

It is, indeed, clear that convection must in time carry some vorticity right away from, or at least right past, the surface. We shall use the word 'wake' to denote the region of vorticity which is not close to the surface. Of this vorticity, the outlying portions are convected downstream at a speed close to U; hence, the wake has a continually increasing length, which prevents the flow as a whole from ever becoming steady. Nevertheless, after a time interval of order $10l/U_\infty$, the further lengthening of the wake, far downstream, has a negligible influence on the flow pattern near the body, which becomes steady as far as changes from this cause are concerned; it is then effectively as if the wake were infinitely long, as in the completely steady flow which we shall principally discuss.

These considerations regarding the two regions of vorticity—boundary layer and wake—indicate the possible existence of a particularly important class of fluid flows. They are what may be called 'thin-wake' flows, in which the boundary-layer thickness remains small, of order $\sqrt{(\nu l/U_\infty)}$, over the whole surface, and the vorticity leaves the surface in a wake of the same order of thickness. Such flows are important largely because, with a thin wake, a body leaves less energy behind in the fluid than with a thick one, and hence its resistance is lower. A second valuable property is that they can be approximately calculated, in three stages (of which just the first two, or even the first alone, may often be regarded as sufficient):

(i) determine the irrotational flow outside the boundary layer and wake, by ignoring the former and replacing the latter by a 'vortex sheet', its mathematical limit as the thickness tends to zero, the total vorticity per unit area remaining unchanged;

(ii) from a knowledge of this external flow, determine the detailed vorticity distribution within the boundary layer, by methods to be described below;

(iii) find the modifications to the irrotational flow due to the calculated 'displacement thickness' of the boundary layer (an effect already explained in a simple special case in Section 2.1).

Although calculations of type (i) are not studied in this book, but

rather in the companion volume *Incompressible Aerodynamics*, we may here mention some of the principal kinds. In steady 'two-dimensional' flow (that is, flow around cylinders, with the same velocity field in each plane perpendicular to the generators), the total vorticity per unit area of wake can be shown to vanish, which leaves for calculation a simple irrotational flow without concentrated vorticity. By contrast, in three-dimensional flows, and also in unsteady flows, the solution requires in general the presence of a vortex sheet, like that behind the trailing edge of a straight wing, or that stretching from the leading edge of a 'narrow delta' wing. The appropriate distribution of total vorticity in such cases follows from the condition of 'smooth flow' at the edge, to be explained in Section 2.5.

Actually, diffusion must thicken the vortex wake far behind the body, and other complications, including its 'rolling up' into discrete vortices, are often neglected in the theory, but, as already remarked, the detailed distribution of vorticity far behind the body has little effect on the flow near it, and hence on the aerodynamic forces. These may to good approximation be divided into those present in the irrotational-flow calculation (i) (these include 'lift' and 'induced drag', and are closely related to the distribution of total vorticity in the wake), and those due to the boundary layer, namely, skin-friction forces deducible from calculation (ii), and extra pressure forces, whose calculation in principle requires (iii) as well as (ii), but whose resultant can be inferred from (ii) alone.

We must now ask: under what circumstances do such thin-wake flows occur? This leads to the general question of how boundary layers separate from solid surfaces, and, through it (as we shall see) to the still more general question of how vorticity distributes itself in steady laminar boundary layers. All these questions are now discussed, first in the simple particular case of 'two-dimensional' flow, and then in the general case.

2.3. *Two-dimensional flows; attachment and separation*

The greatest simplifying feature of two-dimensional flow about an infinite cylinder of arbitrary cross-section is that all vortex lines are parallel to the generators of the cylinder at all times; because, physically, any spin must be about this direction, or, mathematically, choosing the y-axis parallel to the generators, we have $v_y = 0$, v_x and v_z independent of y, and hence, by (1), $\omega_x = \omega_z = 0$ and ω_y independent of y. Convection of the vortex lines cannot therefore stretch or rotate them, so that

values of ω (where for brevity the suffix y is henceforth dropped) are convected without alteration except that due to diffusion—just like values of (say) temperature.

It must be admitted that this and other simplifying features have tempted theoretical hydrodynamicists into an unwarrantable concentration on two-dimensional flows, leading experimentalists to similar restrictions for the sake of comparison with theory. Actually, reproduction of these flows is not easy, as in a real flow the 'straight parallel vortex lines' must form parts of closed loops (Section 1.2) by turning at their ends—either on the side walls of a wind-tunnel, where they can generate complicated 'secondary flows', or else as trailing vorticity (behind finite cylinders), with power to change the whole velocity field. In the meantime, the huge class of motions that depend crucially on the stretching and rotation of vortex lines have been inadequately studied; accordingly, we must hasten to resume three-dimensional theory after the following preliminary discussion of the two-dimensional case.

The most important question is whether the boundary-layer thickness remains small, of order $\sqrt{(\nu l/U_\infty)}$, or whether this diffusion distance is far exceeded by the effect of convection in separating vorticity from the surface. We must ask, therefore: how parallel to the surface are the neighbouring streamlines? The answer can be given in terms of ω_w, the vorticity at the surface. It is easy to see that, at a very small distance z from the surface, the velocity has components $\omega_w z$ parallel to the surface (in a clockwise direction, if ω, the vorticity, is measured clockwise) and $-\frac{1}{2}\omega'_w z^2$ normal to it (where the prime signifies differentiation along the surface, also in the clockwise direction). Accordingly, the direction of streamlines very close to the surface (that is, where z is very small) is almost parallel to it, unless $\omega_w = 0$. Indeed, along any such streamline,

$$\tfrac{1}{2}\omega_w z^2 = \epsilon, \tag{12}$$

the constant ϵ being the volume flow per unit span between the streamline and the surface. Hence, the distance z from the surface varies like $\omega_w^{-\frac{1}{2}}$, which implies only a moderate variation except where ω_w approaches zero.

Points on the surface where $\omega_w = 0$ and $\omega'_w < 0$ (giving a positive velocity component $-\frac{1}{2}\omega'_w z^2$ normal to the surface) are called points of separation; conversely, points where $\omega_w = 0$ and $\omega'_w > 0$ are called points of attachment. That at such points streamlines come right away from the surface is indicated by the flow direction failing to become

tangential as $z \to 0$, as well as by equation (12). However, this equation loses accuracy seriously as $\omega_w \to 0$, and needs to be supplemented with the z^3 term in the expansion of the volume flow in powers of z, giving

$$\tfrac{1}{2}\omega_w z^2 + \frac{1}{6}\left(\frac{p'_w}{\mu} - \kappa\omega_w\right) z^3 = \epsilon, \tag{13}$$

where p_w is the pressure at the surface and κ its curvature. Solutions of equation (13) for z remain small, and close to $\sqrt{(2\epsilon/\omega_w)}$, except near

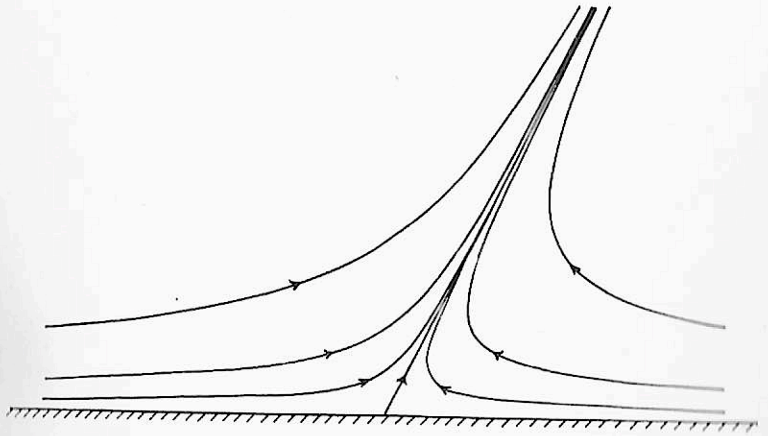

FIG. II. 5. Streamlines near a point of separation. (For those near a point of attachment, reverse all arrows.)

points of attachment or separation, where they cease to be small. The limit as $\epsilon \to 0$ of these solutions is a 'dividing streamline', which at each such point leaves the surface, at an angle (measured clockwise from it) of $\tan^{-1}(3\mu\omega'_w/p'_w)$, the flow thereon being towards the surface at a point of attachment and away from it at a point of separation (Fig. II. 5).

Around the cross-section of the cylinder there must be an even number of points where $\omega_w = 0$, which are alternately points of attachment and of separation. If several points of attachment exist, at most one of the streamlines dividing at them can come from far upstream (since, if two did, then the separation streamline which must lie between them would involve back flow far upstream, which is impossible). Apart from this 'first' point of attachment (of a streamline from far upstream), the others are points of attachment of streamlines that have left the surface at points of separation, enclosing 'bubbles' of various forms (see Fig. II. 6, in which points of attachment and separation are

marked A and S respectively). These flows are not thin-wake flows, as vorticity is convected and diffused throughout the bubble in each case. Note that a thin boundary layer exists only between the first attachment point and the two nearest separation points, which accordingly are the points of 'boundary-layer separation'.

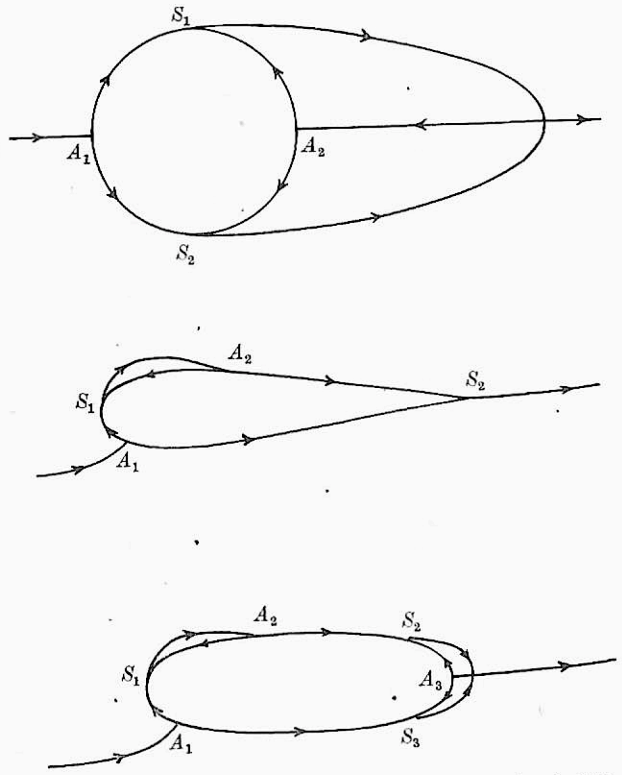

FIG. II. 6. Illustrating different forms of separation bubble.

If, however, there is only one attachment point, and hence only one separation point, then the boundary layer covers the whole surface, from which vorticity is convected away only at the final separation point, where the volume flow of rotational fluid is small, yielding a thin wake. (At the same time, since 'thin' is a relative term, we must admit that a thin wake is possible also if, say, two separation points and a second attachment point are extremely closely clustered together at the rear of the cylinder.) At the end of the next section we study the conditions tending to produce boundary-layer separation, whence can be inferred those for thin-wake flows to exist.

2.4. *Two-dimensional boundary-layer theory*

We discuss now the distribution of vorticity in the boundary layer, beginning at the 'first point of attachment', where a streamline from far upstream joins the surface.

We have noted already a tendency for boundary-layer thickness to increase as the distance from this point increases, since the vorticity in the outer parts of the layer has then been diffusing for a longer time. However, this has not inevitably increased its distance from the surface. For example, near the first point of attachment, diffusion away from the surface is combated by convection towards it, along streamlines which converge in this neighbourhood (as the condition $\omega'_w > 0$ implies). If the surface is smooth at this point (that is, exhibits no sharp edge or angle), the streamline convergence is enough to keep the boundary layer locally of uniform thickness, for the flow outside the boundary layer, because it is an irrotational flow near the point where a dividing streamline joins a smooth surface, satisfies approximately

$$w = -\beta z, \tag{14}$$

where w is the velocity component normal to the surface and β is a constant of order U_∞/l. This inflow can exactly balance the speed at which vorticity in the outer parts of the layer diffuses outwards (which after diffusion through distance z is of order ν/z), for a value of z of order $\sqrt{(\nu/\beta)}$. Thus, the boundary-layer thickness is of order $\sqrt{(\nu l/U_\infty)}$, even at the first point of attachment; it may grow with distance from that point as the value of $-\partial w/\partial z$ outside the boundary layer falls off, but not change its order of magnitude. (On the other hand, if attachment occurs at a sharp edge or angle, then the layer grows with distance from a much smaller value at the edge.)

The 'displacement thickness' δ_1 at any point of the surface is defined (Section 2.1) as the mean distance, along the normal from the point, of vortex elements. To a first approximation, these behave as if concentrated in a vortex sheet at distance δ_1 from the surface, whence the irrotational flow outside the boundary layer is the same as the irrotational flow over a solid surface in this position. This means, for example, that (14) should really have read $w = -\beta(z-\delta_1)$, but it is easily seen that this would not have altered the conclusion drawn from that equation. Exact calculation (Chapter V) shows, in fact, that $\delta_1 = 0{\cdot}65\sqrt{(\nu/\beta)}$ in this region.

To proceed farther, it is necessary to consider the actual vorticity source strength per unit area of surface, and to use an approximate

relationship between vorticity and velocity in the boundary layer. This relationship, which is equivalent to the 'boundary-layer approximation' introduced by Prandtl, is

$$\omega = \partial u/\partial z, \tag{15}$$

where u is the velocity component parallel to the surface (in a clockwise direction). In Cartesian coordinates x, z, equation (15) neglects the additional term $-\partial w/\partial x$ in ω, but this is permissible since w is much smaller than u near the surface, and, also, gradients in the z-direction (normal to the surface) are much steeper than those in the x-direction (tangential to it). Actually, the definition of z as distance from the, in general, curved surface makes the coordinate system curvilinear, although it is still *orthogonal* if the x-coordinate of a point P is defined as the distance along the surface between the nearest point on the surface to P and (say) the first point of attachment. The curvilinear character of the system adds a term κu to ω, but this also is small compared with (15) provided that the radius of curvature κ^{-1} of the surface is large compared with the boundary-layer thickness.

Now U, defined as the total vorticity per unit area of boundary layer at a given point of the surface, can be written as

$$U = \int_0^\delta \omega \, dz, \tag{16}$$

if δ is a value of z at the outer edge of the boundary layer. Hence, on the approximation (15), U is the velocity at $z = \delta$; for this reason, it may be called the 'external flow' velocity.

To the same approximation, the rate of convection of total vorticity, per unit span, past a given point of the surface is

$$\int_0^\delta u\omega \, dz = \int_0^\delta u(\partial u/\partial z)\, dz = \tfrac{1}{2}U^2 \tag{17}$$

(which shows that the *mean* velocity of convection is $\frac{1}{2}U$). The variation of this vorticity-flow rate with x can in steady flow be due only to new vorticity, whose rate of creation at the surface is therefore

$$d(\tfrac{1}{2}U^2)/dx = UU' \tag{18}$$

per unit area. This agrees with the formula $-p'_w/\rho$ for a flat surface which follows from Section 1.5, since Bernoulli's equation gives approximately $p + \frac{1}{2}\rho U^2 =$ constant for the external flow, and the pressure varies negligibly across the layer (see Section 2.9). The reason why the finite radius of curvature of the surface makes negligible difference is

that it has been supposed large compared with the boundary-layer thickness.

Now, as the external flow velocity U rises from its value 0 at the first point of attachment to the maximum positive value which it takes on the surface, the vorticity source strength (18) remains positive. Since only positive vorticity is being created, it follows that, whatever convection and diffusion occur, ω must be positive throughout this

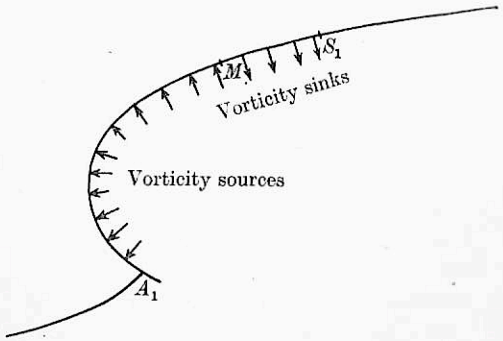

FIG. II. 7. Two-dimensional boundary-layer separation. The vorticity ω is positive (clockwise) throughout the layer in the region of positive vorticity source strength, but, after the strength becomes negative (at M, where the external flow velocity is a maximum), abstraction of vorticity at the surface rapidly reduces the surface value ω_w, which becomes zero at S_1, signifying separation.

part of the layer, where therefore separation (which requires $\omega_w = 0$) is impossible; in fact, ω_w must exceed the values of ω away from the surface, a result which we shall need to remember in Section 3.1. Beyond the maximum of U, however, (18) is negative, so that vorticity is abstracted at the surface (Fig. II. 7). This does not at once bring ω_w down to zero, since reduction of ω_w below the values of ω in the middle of the layer is combated by diffusion in towards the surface. Nevertheless, the surface sink of vorticity succeeds in reducing ω_w to zero when U has fallen to around 95 per cent. of its maximum, so that separation follows fairly hard on the attainment of the maximum external velocity (Chapter VI; the figure quoted is for a typical case, where the negative gradient of U increases continuously beyond the point M; values around 90 per cent. are possible if the gradient is nearly uniform, as this gives inward diffusion more chance).

Where $U' < 0$, the divergence of streamlines in the boundary layer supplements diffusion in producing thickening. Just before separation the thickening becomes particularly marked (Section 2.3), and the

boundary-layer approximations then become inadequate; nevertheless, they have led to reasonable agreement with experiment in predictions of the point of separation.

2.5. *Two-dimensional thin-wake flows*

When the two boundary layers stretching out on either side of the first point of attachment separate at points not very close together, there must be a thick wake. The distribution of the external flow velocity U is then strongly influenced by the distribution of vorticity in the wake, and cannot be calculated in advance (even approximately) from irrotational-flow theory.

This would make boundary-layer theory, in which U, as we have seen, is supposed known, of little value, if it were not that the main *practical* requirements from it are a condition for the existence of thin-wake flows and a technique for calculating them. Now, if thin-wake flow is possible, the external flow velocity U is approximately that for irrotational flow around the cylinder. Hence the requirement, that (at least 'till the last moment') separation does not occur, exacts that the surface velocity in that irrotational flow fall only a few per cent. below its maximum.

Conversely, if the irrotational distribution of external flow velocity satisfies this condition for the absence of premature separation, then it is impossible, when the motion is started from rest, that any flow but the thin-wake flow be set up. For, if separation cannot occur in the steady state, then also it cannot earlier, when it is more effectively combated by inward diffusion because the boundary layer is thinner.

Now, the stated condition on the surface velocity distribution in the irrotational flow around the cylinder can be exactly satisfied only if the cylinder ends in a cusped 'trailing edge', where such a flow commonly departs from the surface at a velocity only a little below that of the undisturbed stream (whereas dividing streamlines can leave *smooth* surfaces only at stagnation points). However, this trailing-edge velocity is sufficiently near to the maximum of U only if the dimensions of the cylinder at right angles to the stream are much less than those parallel to it. This indicates the importance of 'aerofoil' sections—thin shapes with cuspidal trailing edges. Even with these, extreme slenderness would be required to satisfy the condition of no premature separation of a laminar boundary layer (for example, the thickness-chord ratio of a 'Joukowsky' aerofoil, even in symmetrical flow, would need to be 5 per cent. or less). Fortunately, the transition to turbulence,

which we shall see occurs in all practical aerofoil flows, delays separation sufficiently so that this requirement on slenderness is made considerably less extreme.

A cusped edge is inacceptable in a practical structure, but a thin-wake flow is still attainable with various 'near-cusped' shapes, such as that obtained by rounding off the tip of the cusp. A sharp-angled trailing edge is also acceptable; although irrotational-flow separation

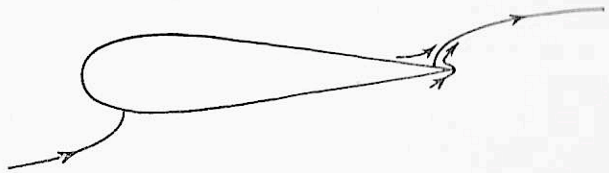

FIG. II. 8. Irrotational flow about an aerofoil.

from it does require it to be a stagnation point, the velocity on that theory falls to zero only very abruptly and 'at the last moment' (like the $\alpha/(2\pi-\alpha)$th power of the distance from the edge, where α is its angle); this may well produce separation only close to the edge, and, in any case, the true variation of the external flow is made less extreme by the displacement effect of the boundary layer.

Clearly, thin-wake flow can occur only if the aerofoil has an appropriate attitude to the oncoming stream. Indeed, irrotational-flow theory tells us that, except in one particular attitude, the dividing streamline does not leave the surface at the trailing edge, but at a stagnation point just ahead of the edge, the velocity at the edge itself being 'infinite' (Fig. II. 8). It is clear that, of the two boundary layers approaching the stagnation point in this case, the one approaching it from behind must separate at a higher value of the external flow speed U, and hence also of the vorticity flow rate (17). Therefore, in the case illustrated in the figure, negative (that is, anticlockwise) vorticity is 'cast off' into the wake.

Now, the presence of such negative vorticity behind the aerofoil alters the flow about it in such a way as to bring the stagnation point nearer the trailing edge. This consideration leads to the Kutta–Joukowsky hypothesis, that such vorticity will continue to be cast off until the flow about the aerofoil in the presence of the wake vorticity leaves the surface 'smoothly' at the trailing edge. The success of the two-dimensional-aerofoil theory for unsteady flows (e.g. with oscillating aerofoils), where one supposes the vorticity in the wake concentrated into a plane vortex sheet, adjusting itself with zero delay time to the requirement

of smooth flow at the trailing edge, indicates that such adjustment is in fact very rapid.

In steadily maintained flow, the total cast-off vorticity tends in due course to a limit, say, $-K$, and all this vorticity departs far downstream. Near the body we have, then, a steady flow with no net wake vorticity but total boundary-layer vorticity $+K$ (because, in two-dimensional flow, convection and diffusion cannot alter the total vorticity of the fluid). Outside the boundary layer this flow is approximately the irrotational one around the aerofoil 'with circulation K', whence K may be determined by the condition of smooth flow at the trailing edge; more accurately, this condition (with 'smooth flow' interpreted to mean equal external-flow velocity on both sides of the aerofoil, yielding zero total vorticity discharge into the wake) should be applied to the external flow as modified by the boundary-layer displacement thickness. The 'lift' on the aerofoil per unit span is then close to $\rho U_\infty K$, attainable values of the lift being limited by the requirement that the flow with circulation K must be such that premature separation is avoided.

These matters are discussed further in the companion volume *Incompressible Aerodynamics*, while there will be some further discussion of two-dimensional flows in general in Section 4.

2.6. *Attachment and separation in three-dimensional flows*

We return now, in the general three-dimensional case, to the question, 'does the boundary-layer thickness remain small, of order $\sqrt{(\nu l/U_\infty)}$?', which, as we have seen, involves the question, 'how parallel to the surface are the neighbouring streamlines?' Strong indications of the answer are again given by the distribution of $\boldsymbol{\omega}_w$, the vorticity at the surface (which in general is a *vector*, tangential to the surface, not as in Section 2.3, where ω stood for the single non-zero component ω_y).

At a very small distance z from the surface, the velocity is approximately

$$\mathbf{v} = \boldsymbol{\epsilon}_w z, \tag{19}$$

where

$$\boldsymbol{\epsilon}_w = \boldsymbol{\omega}_w \times \mathbf{n} = \boldsymbol{\tau}_w/\mu \tag{20}$$

is the vector $\boldsymbol{\omega}_w$ turned through 90° (in the negative sense, about the outward normal $\mathbf{n}$ from the surface), and $\mu\boldsymbol{\epsilon}_w = \boldsymbol{\tau}_w$ is the viscous force on the surface per unit area, or 'skin friction'. Expression (19) for the velocity, neglecting terms in z^2, is tangential to the surface, but from it one can deduce a first approximation, of order z^2, to the normal component of velocity w. For, by solenoidality, $\partial w/\partial z$ must be minus the two-dimensional divergence of $\boldsymbol{\epsilon}_w z$ for very small z. Hence,

$$w = -\tfrac{1}{2}\Delta z^2, \tag{21}$$

where Δ is $\operatorname{div} \boldsymbol{\epsilon}_w$, with $\boldsymbol{\epsilon}_w$ regarded as a two-dimensional vector field; Δ is also related directly to $\boldsymbol{\omega}_w$, being the surface value of the normal component of $\operatorname{curl} \boldsymbol{\omega}$.

We see from (19) and (21) that the direction of streamlines as $z \to 0$ becomes parallel to the surface, except where $\boldsymbol{\epsilon}_w = 0$, or, what is the same thing, $\boldsymbol{\omega}_w = 0$. This condition, that both tangential components of vorticity vanish simultaneously, is satisfied in general only at isolated points of the surface, which we call 'points of separation' if $\Delta < 0$ (so that the normal velocity (21) is positive) and 'points of attachment' if $\Delta > 0$ (Legendre 1956). It is only in quite exceptional circumstances, usually owing to some kind of symmetry, that $\boldsymbol{\omega}_w = 0$ all along a line; these include, however, the case of ideal two-dimensional flow (note that when such flow is thought of as 'in two dimensions', we refer to *points* of attachment, etc., but that, when it is seen as a three-dimensional flow around an infinite cylinder, such a 'point' becomes a whole generator of the cylinder, that is, a line of attachment at right angles to the stream). Again, in axisymmetrical flow about a body of revolution, symmetry produces whole lines of separation or attachment, in this case circles coaxial with the body. However, any slight change to either of these situations, such as cropping the cylinder or yawing the body, retrieves the general case, in which $\boldsymbol{\omega}_w = 0$ only at isolated points.

In this general case, the character of the flow near the surface can, to a large extent, be inferred from the surface pattern of 'skin-friction lines' (curves to which $\boldsymbol{\epsilon}_w$ is everywhere tangential, so that the skin-friction vector $\boldsymbol{\tau}_w = \mu\boldsymbol{\epsilon}_w$ also is) and of vortex lines. Both these systems of lines cover the surface completely, crossing each other everywhere at right angles. The pattern of skin-friction lines can often be approximately determined by an experimental technique, described in Chapter X, in which the surface is covered with an oily substance, which leaves permanently visible streaks behind it when the skin-friction force causes it to flow along those lines.

Streamlines very near to the surface lie closely along the skin-friction lines, as (19) indicates (for this reason they are sometimes called 'surface streamlines' or 'limiting streamlines'); however, their distance z from the surface varies, not as $\omega_w^{-\frac{1}{2}}$ (see equation (12)), but as $(\omega_w h)^{-1}$, where h is the distance between two adjacent skin-friction lines. This is because

in a streamtube of rectangular section, whose base is the portion of surface between the two skin-friction lines and whose (variable) height is z, we have

$$\tfrac{1}{2}\omega_w z^2 h = \epsilon, \tag{22}$$

where ϵ is the volume flow along the streamtube, and ω_w is the magnitude of $\boldsymbol{\omega}_w$ (and of $\boldsymbol{\epsilon}_w$). It follows that streamlines can increase greatly their distance from the surface, not only where ω_w becomes very small, but also where h does, that is, where skin-friction lines run very close together. These alternative mechanisms of separation need to be borne continuously in mind.

There is just one skin-friction line and one vortex line through each point of the surface, except a point of attachment or separation (where $\boldsymbol{\epsilon}_w = \boldsymbol{\omega}_w = 0$). These last are 'singular points' of the differential equations of both systems of curves (namely, the equations $d\mathbf{r} \| \boldsymbol{\epsilon}_w$ and $d\mathbf{r} \| \boldsymbol{\omega}_w$, respectively, where $d\mathbf{r}$ is the relative position of two adjacent points on a curve). Such singular points are classified by mathematicians into two main types (see, for example, Kaplan 1958, chapter 11), depending on the sign of the 'Jacobian',

$$J = \frac{\partial \omega_x}{\partial x}\frac{\partial \omega_y}{\partial y} - \frac{\partial \omega_x}{\partial y}\frac{\partial \omega_y}{\partial x} = \frac{\partial \epsilon_x}{\partial x}\frac{\partial \epsilon_y}{\partial y} - \frac{\partial \epsilon_x}{\partial y}\frac{\partial \epsilon_y}{\partial x}, \tag{23}$$

where the suffices denote components of $\boldsymbol{\omega}_w$ and $\boldsymbol{\epsilon}_w$ in the x- and y-directions, and x, y, z are Cartesian coordinates with origin O at the singular point and Oz normal to the surface.

A singular point where $J < 0$ is a 'saddle point' (of attachment or separation according as $\Delta > 0$ or $\Delta < 0$). Near a saddle point the pattern of skin-friction and vortex lines is as in Fig. II. 9, where the arrows indicate the direction of $\boldsymbol{\epsilon}_w$, and hence also of streamlines very close to the surface.

A singular point where $J > 0$, however, is a 'nodal point'. Fig. II. 10 indicates a number of possible surface patterns near nodal points of attachment, with arrows meaning the same as before. The inequalities under the patterns give, in terms of J and of

$$\Delta = \operatorname{div} \boldsymbol{\epsilon}_w = \frac{\partial \epsilon_x}{\partial x} + \frac{\partial \epsilon_y}{\partial y} = \frac{\partial \omega_y}{\partial x} - \frac{\partial \omega_x}{\partial y},$$

$$\Omega = \operatorname{div} \boldsymbol{\omega}_w = \frac{\partial \omega_x}{\partial x} + \frac{\partial \omega_y}{\partial y}, \tag{24}$$

the condition for each type to occur; cases of equality, however, are not exhibited, except for the case $\Omega = 0$, which we shall see is of special

importance, since it occurs at any nodal point of attachment of a streamline from far upstream. From each type of nodal point an infinite number of skin-friction lines emerge, either having all (except one) the

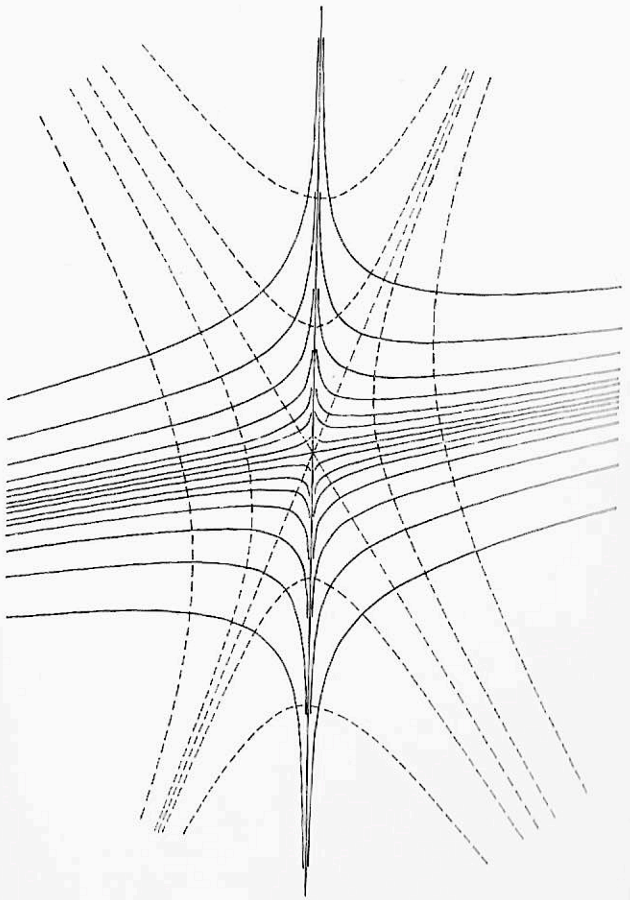

FIG. II. 9. Typical pattern of skin-friction lines (full) and vortex lines (broken) near a saddle point.

same tangent, or else spirally. Spiral attachment occurs principally when either the surface or the external flow is rotating, as, for example, in flows studied in Section III. 20.

The possible local patterns at a nodal point of separation are exactly the same as in Fig. II. 10, but with all the arrows reversed. Spiral separation, however, can occur even in ordinary flows over sweptback wings, when oil is sometimes seen to accumulate at a point and spin around (see Garner and Bryer 1959 and Fig. II. 14 below).

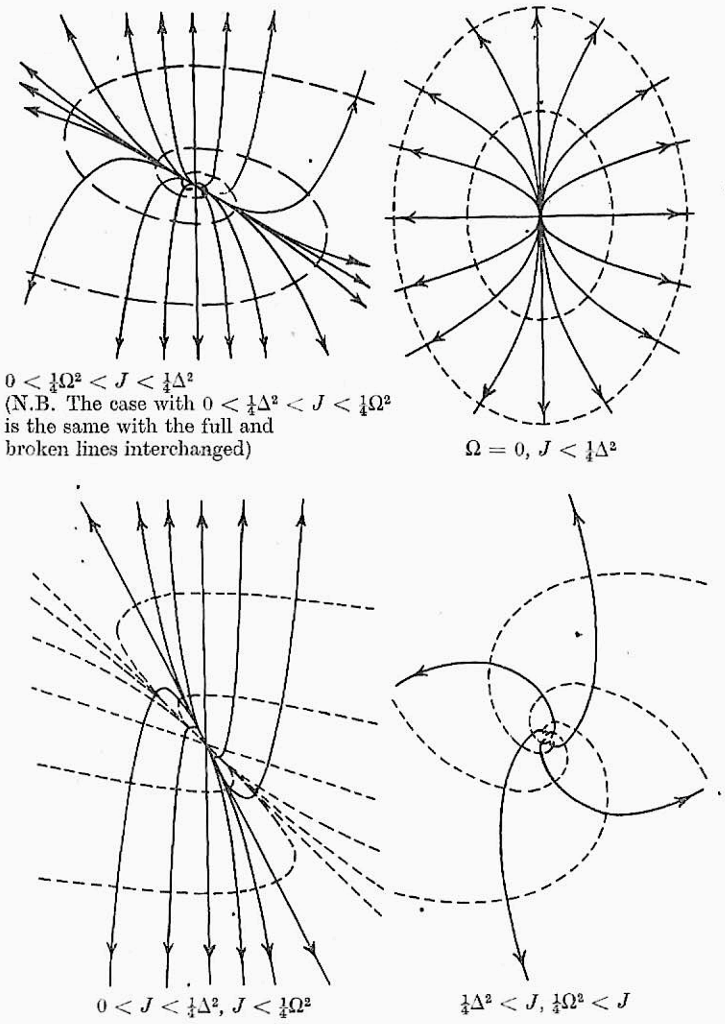

FIG. II. 10. Different types of pattern of skin-friction lines (full) and vortex lines (broken) near a nodal point of attachment ($J > 0, \Delta > 0$).

2.7. *Topography of skin-friction lines and vortex lines*

The range of possible overall patterns of skin-friction and vortex lines on a smooth surface is subject to a topological law, that the number of nodal points must exceed the number of saddle points by 2 (see for example Kaplan 1958, p. 444, or Coddington and Levinson 1955, chapter 16).

To get a physical 'feel' for this law (whose mathematical proof, from properties of the Jacobian (23), is not extremely recherché, but would

be out of place here), one may argue that the infinity of skin-friction lines on the surface must begin and end somewhere, which indicates that there is at least one nodal point of attachment and one nodal point of separation. If there are *two* nodal points of attachment, the skin-friction lines from each must somewhere run into one another, and so have to divide at a saddle point. Fig. II. 11 shows that this combination, of two nodal points of attachment and a saddle point (whether of attachment or separation), is similar to a single nodal point of attachment in being a simple 'source' of skin-friction lines; the same is true of n nodal points of attachment and $(n-1)$ saddle points. Similarly, m nodal points of separation and $(m-1)$ saddle points behave like a 'sink', into which skin-friction lines issuing from the 'source' can disappear, giving a possible arrangement of such lines with $m+n$ nodal points and $m+n-2$ saddle points. Actually, the most general arrangement is of the form just described, except when $\Delta = 0$ at some nodal points, whose total number, even then, must exceed by 2 that of the saddle points.

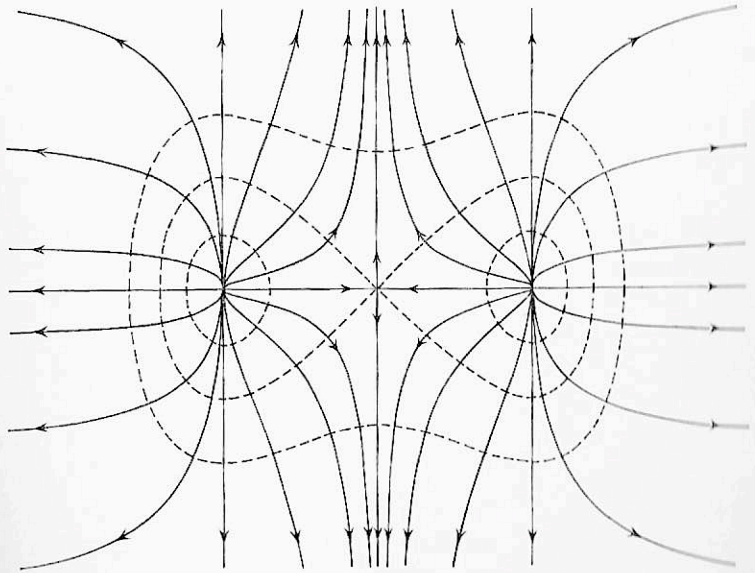

FIG. II. 11. A combination of two nodal points of attachment and one saddle point.

A feature of three-dimensional flow is that there can be any number of nodal points of attachment of streamlines from far upstream. This is true even for ideal irrotational flow, in which a body with (say) two

protuberances in front has normally a stagnation point on each; these are nodal points of attachment of irrotational-flow streamlines, and somewhere between them is a third stagnation point, which is a saddle point of attachment (such as may occur in practice on a wing leading edge between two engine nacelles). The real flows about bodies of this kind have points of attachment close to those given by irrotational-flow theory, any differences being due mainly to wake-induced flow. Fig. II. 11 shows a typical surface pattern over the front; note that, as no vortex line attaches itself to the surface at these points of attachment of streamlines from far upstream, the surface vortex lines in their neighbourhood are closed (compare Fig. II. 10 for the case with $\Omega = 0$).

At any nodal point of attachment of fluid which has not previously acquired vorticity, the boundary-layer thickness is determined, as in Section 2.4, by a balance between diffusion of vorticity out from the surface and convection inward; the external flow normal to the surface being (as before) of the form $w = -\beta z$, or $w = -\beta(z-\delta_1)$ if the displacement-thickness effect is taken into account. This argument again suggests a thickness of order $\sqrt{(\nu/\beta)}$, and calculation has shown that δ_1 is between $0{\cdot}65\sqrt{(\nu/\beta)}$ and $0{\cdot}80\sqrt{(\nu/\beta)}$ for all such nodal points (Howarth 1951*c*). Calculations have not been made for the full range of saddle points of attachment, but the same arguments apply, however surprising this may seem in view of the far greater stretch of surface which has been traversed by some of the fluid near a saddle point. The reason is that, even if this fluid was formerly in a much thicker boundary layer, it has recently formed part of a layer with $\partial w/\partial z = -\beta$ outside it, for long enough to bring the thickness down to order $\sqrt{(\nu/\beta)}$.

Departure from the surface of the vorticity in a boundary layer, which has originated as just described from one or more points of attachment, occurs commonly at a 'line of separation'. This is defined as a skin-friction line which issues from both sides of a saddle point of separation and, after embracing the body, disappears into a nodal point of separation. A line of separation partitions the surface; only the skin-friction lines ahead of it have originated at the forward points of attachment, while those behind have issued from a nodal point (or points) of attachment at the rear. Note that it may or may not be 'wake fluid' (with previously acquired vorticity) that becomes attached at such a rear point, but that, if it is, then a wider range of surface patterns is possible there than at the nodal points of attachment just mentioned.

The twofold mechanism of separation, referred to in Section 2.6, is clearly exhibited at lines of separation. Streamlines depart from the

surface, not only because ω_w falls to zero as either point of separation is approached, but also because the surface topography near a saddle point is such as to make streamlines come close together along the line of separation, whence the h of equation (22) falls greatly as they approach it. The apparently rather extreme case of this running together exhibited in Fig. II. 9 is by no means atypical of surface patterns inferred from oilflow photographs, which have led some writers to speak

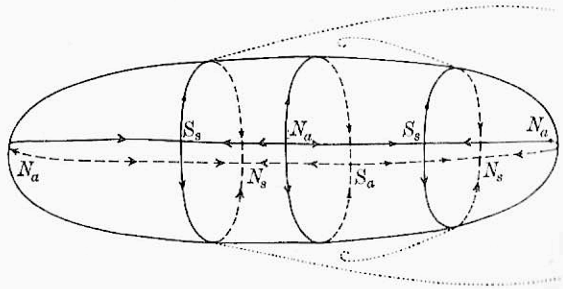

FIG. II. 12. Possible pattern of skin-friction lines on a smooth surface (of which the full and broken lines are on the near and far sides, respectively). N and S signify nodal and saddle points, and subscripts a and s attachment and separation. The dotted lines suggest what happens to fluid separating at the primary and secondary lines of separation.

of skin-friction lines as 'running tangentially into', or 'having cusps on' a line of separation (Maskell 1955). These statements have often very considerable approximate validity, although to go on and call the line of separation an 'envelope' of skin-friction lines is confusingly inaccurate.

The main ingredients of skin-friction-line topography on a smooth surface have now been described. Fig. II. 12 illustrates a further combination of them, in which the backflow towards the line of separation of the boundary layer suffers a 'secondary separation' before reaching it. Note that the law regarding numbers of nodal and saddle points is satisfied.

On surfaces with sharp edges or pointed tips, the topography can be somewhat different. To be sure, the edge or tip is in practice rounded, so that the general theory is correct provided that the detailed pattern in the rounded portion of the surface is included; but such a microscopic view is inconvenient, and one prefers usually to speak of what is left when that small portion of surface is ignored.

The lifting wing with cusped trailing edge is an example whose importance is obvious from Section 2.5 and from practical considerations.

With small enough thickness-chord ratio and angle of incidence, the boundary layer on such a wing may avoid separation altogether, leaving the trailing edge smoothly to form a thin vortex wake. To relate this to the general theory, note that, with a rounded trailing edge, there would be a line of separation around its shoulder, issuing from a saddle point of separation on the lower surface, travelling out to the wing tip,

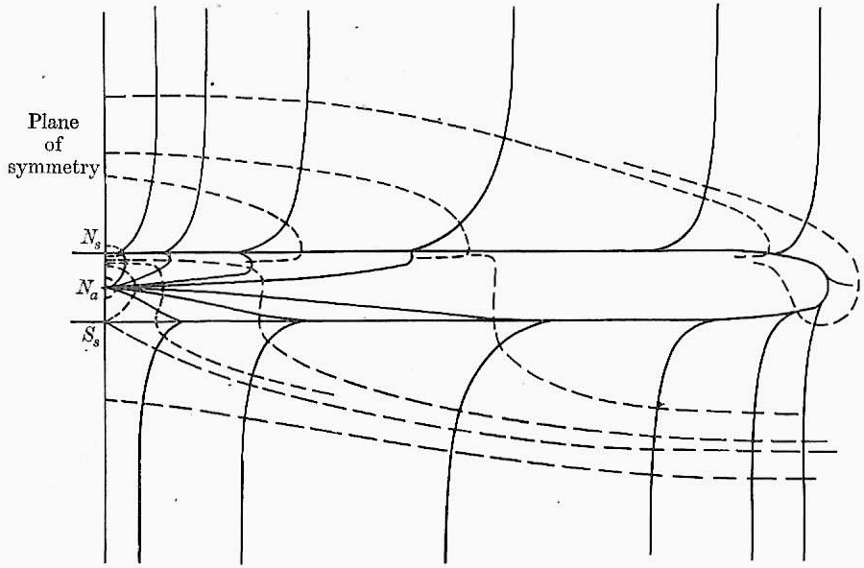

FIG. II. 13. Surface pattern near a rounded trailing edge in thin-wake flow about a lifting wing. (View upstream from behind the trailing edge, with the vertical scale very greatly enlarged.)

and returning along the upper surface to disappear into a nodal point of separation. This contrary motion generates the trailing vorticity, and indeed Fig. II. 13 shows how the surface vortex lines would turn into the downstream direction just before separation.

With other wings or angles of incidence, separation occurs ahead of the trailing edge, and the flow pattern on this smooth part of the surface can show all the features already discussed. Attachment may occur at the trailing edge if there is a line of separation ahead of it. Such attachment would conform to the general theory (taking place at a nodal point, etc.) only if the edge were rounded; if it is cusped, skin-friction lines can become attached all along it.

The line of separation on a stalled wing may lie right along the upper surface of the leading edge, but when only the tips are stalled it issues from a saddle point of separation in a part-span position,

whence one branch travels to the tip while the other travels back to the trailing edge, or sometimes to a spiral point of separation, in both cases shedding a 'part-span vortex sheet' (Fig. II. 14).

The needs of supersonic aircraft have given prominence to the slender 'conical' wing shape, in the general sense of a surface generated by any set of straight lines stretching back from an apex. In certain attitudes,

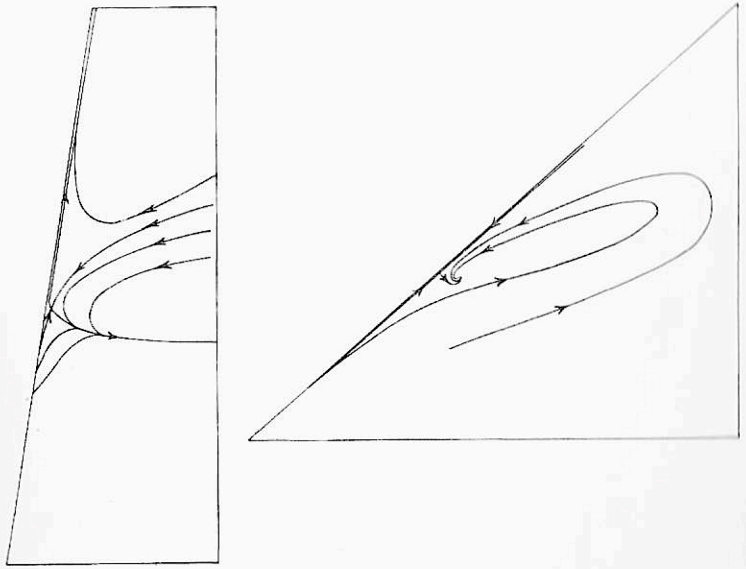

FIG. II. 14. Types of surface pattern for a wing with the tip stalled (straight wing on the left, sweptback wing on the right).

the sharp apex is simply a nodal point of attachment, and the general theory applies; but, at higher angles of incidence, the surface pattern is that generated by two nodal points of attachment and a saddle point of separation which have coalesced at the apex (but would be distinct if the apex were rounded). Such a surface pattern is illustrated in Fig. II. 15. The line of separation S is well marked in oilflow photographs. The almost straight skin-friction line A through the second nodal point of attachment, although less closely defined, has been called a 'line of attachment'. In many such flows the boundary layer is thin enough, except near S, for a thin-wake theory, in which the twirled conical vortex wake which leaves the surface there is suitably approximated, while the flow is regarded as irrotational outside it, to have reached reasonable agreement with experiment (Mangler and Smith 1959). More examples of flow patterns of practical interest are given in Section 26,

in Chapter VIII, and in the companion volume *Incompressible Aerodynamics*.

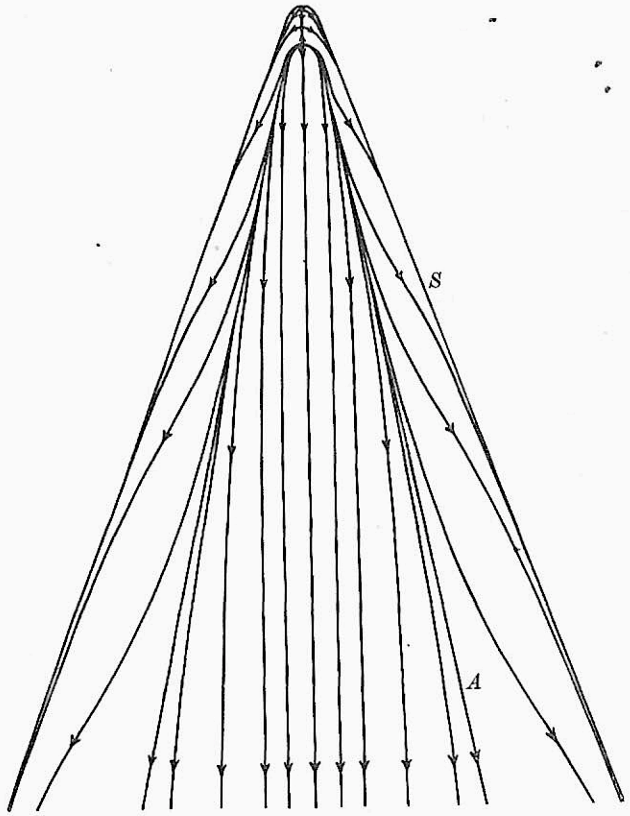

FIG. II. 15. Upper-surface pattern for flow about a 'conical' wing shape at incidence, with apex rounded to show how this splits the singularity there into three.

2.8. *Three-dimensional boundary-layer theory*

The boundary layer in axisymmetrical flow about bodies of revolution has been much investigated. The results are extremely similar to those for two-dimensional flow. This is principally because the vorticity source strength per unit area is the same; modifications to the arguments leading to (18) cancel out, since the additional flow of total vorticity, called for by the additional area (normal to the direction of motion) occupied by vortex elements when they stretch on moving farther from the axis of symmetry, is provided exactly by the dynamical effect of that stretching. Thus, vorticity production and diffusion are unaltered, which, in particular, leaves the condition for separation

almost the same as in two-dimensional flow; the quantitative changes in boundary-layer development, due to modified convective processes, are not great, as is shown in Chapter VIII, Part II, which treats also the case when the body rotates about its axis. Axisymmetrical flow has some attractions if precise comparisons with experiment are sought, as being more accurately realizable than two-dimensional flow and equally amenable to calculation.

By contrast, the quantitative theory of general three-dimensional flow in boundary layers is pitifully undeveloped (Chapter VIII, Part III). Accordingly, we are able here to give only a crude qualitative picture of the factors influencing the vorticity distribution, both through the layer and over the surface, of which the latter has been shown (Sections 2.6 and 2.7) to regulate separation. We shall see that, although the *stretching* of vortex lines has just been found to be relatively immaterial, their *rotation* is of the first importance.

As discussed in connexion with equations (15) and (16), vorticity components are to a good approximation gradients normal to the surface of tangential velocity components, and the total vorticity per unit area of boundary layer, namely

$$\int_0^\delta \boldsymbol{\omega}\, dz = \mathbf{n}\times\mathbf{U}, \tag{25}$$

can be regarded as the external flow velocity, say $\mathbf{U}$, turned through 90° (in the positive sense, about the outward normal $\mathbf{n}$ from the surface). Thus, the mean vortex lines (averaged across the layer) are perpendicular to the surface streamlines of the external flow, and hence lie along the surface equipotentials of that irrotational motion, as vortex lines were noted in Section 2.1 to do exactly in the initial stage of the motion, before convection begins to operate.

Convection tends to alter this distribution of mean or total vorticity, both in magnitude and in direction. To redress the balance, new vorticity is produced at the surface, not only in the direction of the equipotentials, at the rate UU' (the prime signifying gradient along the streamlines), which has already been discussed in special cases, but also (in general) in the direction at right angles, that of the external streamlines, at the rate $\kappa_s U^2$, where κ_s is the curvature of those streamlines in a plane tangential to the surface.

The simplest physical picture of the generation of this so-called streamwise vorticity comes from the idea (Section 2.4) that the 'average velocity of convection' of vorticity is $\frac{1}{2}U$. In time δt this would advance

the vortex lines by $\frac{1}{2}U\,\delta t$, which is *directly* proportional to U; but to lie on an adjacent equipotential, on which the velocity potential is greater by $\delta\phi$, they should have advanced by $U^{-1}\delta\phi$, which is *inversely* proportional to U. Hence, convection makes vortex lines 'lag' most, relative to equipotentials, wherever U is smallest. Fig. II. 16 (which should be read from the bottom upwards) shows this geometrically,

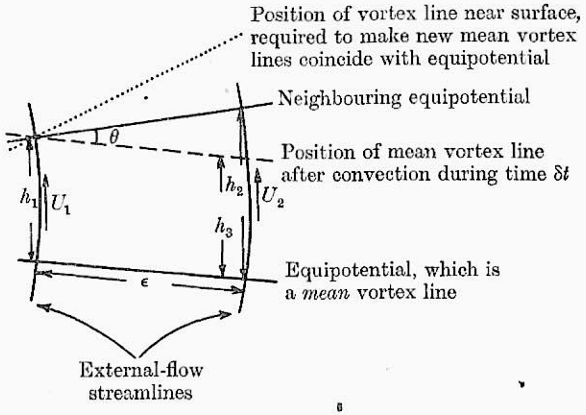

FIG. II. 16. Mechanism of generation of streamwise vorticity. We have $U_1 h_1 = U_2 h_2$, $h_2 = h_1(1+\kappa_s\epsilon)$, $h_1 = \frac{1}{2}U_1\,\delta t$, $h_3 = \frac{1}{2}U_2\,\delta t$, and so the angle

$$\theta = \frac{h_2 - h_3}{\epsilon} = \frac{\frac{1}{2}U_1\,\delta t(1+\kappa_s\epsilon) - \frac{1}{2}U_1\,\delta t(1+\kappa_s\epsilon)^{-1}}{\epsilon} = \kappa_s U_1\,\delta t.$$

indicating that, after a time δt, a vortex line initially along an equipotential arrives at an angle $U\kappa_s\,\delta t$ with the local equipotential; it follows that convection produces total streamwise vorticity $U^2\kappa_s$ per unit area per unit time. This is distributed throughout the layer, while, to balance it, equal and opposite streamwise vorticity is created at the surface. This means that the vortex lines near the surface turn still more rapidly than the equipotentials (as the dotted line in Fig. II. 16 indicates). Note that the distribution of streamwise vorticity through the boundary layer is associated with velocity components perpendicular to the external streamlines and towards their centre of curvature.

A more precise account of vorticity balance gives the same result, that cross-stream vorticity is created at the rate UU' and streamwise vorticity at the rate $U^2\kappa_s$. This can also be directly related (Section 2.9) to the result concerning pressure gradient derived in Section 1.5.

These considerations give one some physical feel for how vorticity distributes itself in boundary layers, explaining why the skin-friction lines tend to curve more exaggeratedly than the external streamlines,

and why the surface vortex lines tend to slew round into a streamwise direction, as near the saddle point of separation in Fig. II. 9. Points of separation themselves tend to be on streamlines that have not curved much on the average (since both components of vorticity must vanish at such points).

We consider now in the general case the effect of the boundary layer on the external flow, which can again be expressed in terms of a displacement thickness δ_1. By redistributing the total cross-stream vorticity U in a vortex sheet at the mean distance δ_c of cross-stream vorticity from the surface, namely

$$\delta_c = \frac{\int_0^\delta z(\partial u/\partial z)\,dz}{\int_0^\delta (\partial u/\partial z)\,dz} = \frac{\int_0^\delta (U-u)\,dz}{U}, \tag{26}$$

where u is the velocity component parallel to the external streamlines, we see that the effect of this vorticity on the irrotational flow outside the boundary layer is to change it into the flow around a surface displaced into the fluid through a distance δ_c. However, the effect of the streamwise vorticity on the external flow is not negligible. Because the total streamwise vorticity across the layer is zero, this vorticity can be thought of as a set of little vortex rings whose axes are equipotentials. But, according to potential theory, a vortex ring is equivalent to a doublet perpendicular to the plane of the ring. It follows that the streamwise vorticity has the same effect as a doublet of strength $U\delta_s$ with axis along an equipotential, where $U\delta_s = \int_0^\delta v\,dz$ and v is the cross-stream velocity in the boundary layer. It may be shown (Lighthill 1958) that these doublets alter the effective displacement thickness from δ_c to

$$\delta_1 = \delta_c - \frac{1}{U}\frac{\partial}{\partial c}\int_{\phi_a}^{\phi} \delta_s\,d\phi, \tag{27}$$

where the integral with respect to the external velocity potential ϕ is along an external streamline from its point of attachment to the surface (namely $\phi = \phi_a$), and where $\partial/\partial c$ signifies differentiation with respect to distance along an equipotential.

We conclude this section by remarking that it is not in every case convenient to resolve the vorticity into the cross-stream and streamwise directions. For example, in the yawed flow past an infinite cylinder,

which is often a valuable idealization of some aspects of the flow over sweptback wings, it is more convenient to work with the 'spanwise' and 'chordwise' components. This is especially so because in this flow the motion of one of the 'arrow-shaped elements of fluid' of Section 1.3 cannot stretch or rotate its spanwise component. (Also, the chordwise component is merely stretched, not rotated.) It follows that the spanwise vorticity distribution, and so also the chordwise velocity distribution, in the boundary layer are the same as in two-dimensional flow, which greatly simplifies the calculation of these flows (Section VIII. 22).

2.9. *Pressure in boundary layers*

The key to understanding complete flows, as we have tried to show, is vorticity theory, which eliminates the pressure as a variable that needs to be considered. However, some knowledge of its distribution is obviously necessary, and may be obtained as follows.

In irrotational flow, the force component in any direction on a fluid element is minus the gradient of the dynamic pressure p_d (Section I. 2.4) per unit volume. This force component equals the mass, ρ per unit volume, multiplied by the component of acceleration in that direction, which may be shown to be the gradient of $\partial\phi/\partial t+\frac{1}{2}v^2$. Hence, the gradient of

$$p_d+\rho(\partial\phi/\partial t+\tfrac{1}{2}v^2) \tag{28}$$

in any direction is zero throughout an irrotational flow, so that (28) must have the same value throughout the flow (Lamb 1932, p. 19). Since the value may vary with time, it is usually written $F(t)$; but for a body moving through otherwise undisturbed fluid we can always take $\phi \to 0$ at infinity, in which case (since $p_d \to 0$ there also) the value of (28) is zero at infinity and so zero everywhere.

Again, in steady flow, with velocity U_∞ at infinity, the uniform value of (28) (where now $\partial\phi/\partial t = 0$) must clearly be $\frac{1}{2}U_\infty^2$, giving

$$p_d = \tfrac{1}{2}\rho(U_\infty^2-v^2). \tag{29}$$

Bernoulli's equation (29) encourages the view of p_d in steady flow as a potential energy per unit volume which on addition of the kinetic energy $\frac{1}{2}\rho v^2$, is conserved if the flow is irrotational (when the non-conservative viscous forces vanish). Constant use of (29) must not, however, seduce one into applying it in unsteady flow without adding the 'transient pressure' $-\rho\,\partial\phi/\partial t$, which can be large (Section I. 2.6). Again, in boundary layers and wakes the flow is not irrotational and (29) cannot be applied, the energy argument suggesting in fact a lower value of $p_d+\frac{1}{2}\rho v^2$ than $\frac{1}{2}\rho U_\infty^2$, owing to viscous dissipation.

To the 'boundary-layer approximation' (Section 2.4), the pressure is constant across the layer. This is simply because the layer is thin, and the gradient of dynamic pressure across it only moderate—approximately $\kappa\rho u^2$, which is the gradient required to make fluid with velocity u follow a body contour with curvature κ. It follows that the dynamic pressure change across the thickness δ is small compared with the value (29) if $\kappa\delta$ is small (as was assumed already in Section 2.4), and therefore, at any point in the boundary layer,

$$p_d \doteq \tfrac{1}{2}\rho(U_\infty^2-U^2), \tag{30}$$

where U is the external flow velocity.

In particular, equation (30) gives the pressure at the surface itself, a result which one might hope to use in 'thin-wake' flows, where the whole surface is covered by boundary layer, to calculate the force on the body. However, the approximation is not good enough for this purpose. Errors, due to neglecting either the pressure gradient across the layer, or the displacement-thickness effect on U, produce a resultant pressure force ('form drag') comparable with the whole viscous force on the body ('skin-friction drag'). Accordingly, such errors cannot be neglected, as often no drag is present from other causes, the pressure forces in pure irrotational flow having zero resultant. Again, in wing aerodynamics, although at high lift the induced drag associated with trailing vorticity may be much greater than the drag due to the boundary layer, it is imperative to know also the drag at zero lift, when this latter component predominates. To get round these difficulties, one does not in practice attempt to calculate surface pressure more precisely, but uses a combination of arguments (Chapter X) in which drag is inferred, from conservation of momentum for large masses of fluid, in terms of the state of the boundary layer at the trailing edge.

We conclude the discussion of pressure in boundary layers with some simple physical arguments for which approximation (30) is adequate. These arguments tell us nothing that has not already been derived more rigorously by vorticity arguments, but they are included because it is useful to be able to view a subject from more than one angle.

From (30), the dynamic pressure gradient parallel to the external streamlines is $-\rho UU'$ at all points of a boundary layer. This gradient (which, according to Sections 1.5, 2.4 and 2.8, is associated with generation of cross-stream vorticity at the rate UU') tends to accelerate the fluid in the boundary layer (which, however, is acted on also by viscous forces) when $U' > 0$, and to retard it when $U' < 0$. In the

latter case, the fluid near the wall (which already is moving only sluggishly) will tend to be brought to rest, leading to separation of the fluid behind it, and the results quoted in Section 2.4 show that this tendency can be withstood by viscous forces to only a restricted extent. This view of pressure forces as tending to produce the (usually unwished-for) separation has led to the phrase 'adverse' pressure gradient being used to denote a rise of pressure (which goes with a fall of velocity) along the external streamlines.

Again, the dynamic pressure gradient perpendicular to the external streamlines is $\kappa_s \rho U^2$ away from their centre of curvature (this 'curvature', and its magnitude κ_s, being curvature in a tangent plane, as in Section 2.8). This result follows directly from (30) and the irrotationality of the external flow, or more simply from considering the centrifugal acceleration of the fluid just outside the boundary layer, and by Sections 1.5 and 2.8 it is associated with generation of streamwise vorticity at the rate $\kappa_s U^2$. Now, the centrifugal acceleration of the much more slowly moving fluid near the surface fails to balance this normal pressure gradient, whence this fluid tends to acquire a velocity component towards the centre of curvature. This is the cross-stream flow, associated with streamwise vorticity, which has been discussed already in Section 2.8.

3. Instability and turbulence

3.1. *Hydrodynamic instability*

We must now refer to the commonplace observation that the flow around a body does not normally develop in a smooth, orderly fashion to a perfectly steady state, as might be expected from Sections 2.1 and 2.2, but that more or less violent, irregular fluctuations appear, especially in the wake. These are ascribed to 'instability' of the flow, that is, the tendency for small disturbances (due to noise, mechanical vibration, surface roughness, non-uniformity of the oncoming stream, etc.) to be amplified into substantial fluctuations. As a result, the final, 'turbulent', motion is at most 'statistically steady', in the sense that the fluid velocity at each point varies about a constant mean value.

The instability can be viewed as an instability of the vorticity distribution, as this fixes the flow field (Section 1.6). We must suppose, therefore, that a very slight displacement of some vorticity, or the creation at the surface of a very little extra vorticity, may induce slight changes in the velocities of convection of existing vortex lines, such that resulting changes in the vorticity pattern a short time later

induce alterations in the velocities of convection of that vorticity pattern, such that, etc., etc.,..., the whole altered process of convection, production and diffusion of vorticity tending more and more to depart from what it would have been without the original disturbance. This supposition would explain why the greatest unsteadiness is found in the wake, the boundary layer, and irrotational-flow regions close enough to these to partake strongly of the motions which are induced by their vorticity fluctuations. In fact, although turbulence is observed most frequently in wakes, it was found soon after the discovery of the boundary layer (Prandtl 1914) that parts of it (at least) are turbulent in a wide range of flows.

In this Section 3, the properties of the initial flow instability, of the ultimately resulting turbulent motion, and of the transition between them, are sketched as briefly as will allow us in Section 4 to give a general picture of the variation of flow patterns with Reynolds number. This material is needed in a work on laminar boundary layers, both to show when and how they fit into flows in general (other parts of which may be turbulent), and to relate the theory of their stability (Chapter IX) to the characteristics of observed motions.

Since diffusion by itself is a stable process, the vorticity distribution is necessarily stable when it dominates sufficiently over convection. By comparing a diffusion rate of order $\nu\omega_0/\delta$, where ω_0 is a typical vorticity and δ the thickness of a layer across which ω varies from 0 to ω_0, with a convection rate of order $U\omega_0$ (both per unit area), we see that stability may be expected if

$$R_\delta = U\delta/\nu \tag{31}$$

is small enough. This gives already a reason why the wake is often observed to be unstable when the boundary layer, or, perhaps, the thinner part of the layer (say, the region of accelerating external flow), is not. However, two effects conspire here; not only is the value of δ less in the region of accelerating external flow, but also, as we shall see, the stability of this part of the layer persists up to considerably higher values of R_δ itself. Meanwhile, we note that the order of magnitude of δ in a boundary layer (Section 2.2) shows that R_δ is of order $\sqrt{(Ul/\nu)} = R^{\frac{1}{2}}$, and, also, that experiment has confirmed the stability of all kinds of flow at sufficiently low Reynolds number.

The stability theory is a mathematical construction of great complexity and beauty, due principally to Tollmien (1929, 1935), although details that help to complete the picture have been contributed by

very many workers. In it, one considers small sine-wave disturbances to a simple vortex layer of uniform thickness, and investigates their distribution across the layer, their phase velocity c_r, and their rate of amplification (positive, negative or zero) with time. Note that, as wave theory tells us, even a localized disturbance can be considered as a combination of such sine waves, although the part of the disturbance with wavelength around the value λ will travel along, not at the speed c_r of its individual crests, but at its 'group velocity' $c_r - \lambda\, dc_r/d\lambda$.

The most important results are as follows:

(i) If, as a first approximation, diffusion and the production of new vorticity are neglected (as in inviscid flow theory), then the waves can have positive rate of amplification only if the undisturbed vorticity distribution has a maximum in the midst of the layer (Tollmien 1935; see also Görtler 1940*a*). On this simplified theory, boundary layers in an accelerating external flow are stable, because in them the maximum vorticity is always at the wall (Section 2.4). On the other hand, boundary layers in retarded flow are unstable, and so are wakes (in which the vorticity must have maxima since it vanishes at the centre); in both these, the rate of amplification is positive for a large band of wavelengths.

(ii) This simplified theory, although making an important distinction, is not accurate enough; in particular, for boundary layers in accelerating flow, the actual predicted wave system (with zero amplification rate) has some seriously unrealistic features, due to the total neglect of the production and diffusion of vorticity. Furthermore, when these are reintroduced, with R_δ finite but still large (slight diffusion), they do not for all wavelengths reduce the amplification rate to negative values; there is, rather, a small band of waves (whose length is a rather large multiple of the layer thickness) the modifications to which cause the amplification rate to become positive (Tollmien 1929, Lin 1945). Accordingly, such a boundary layer is unstable to disturbances of frequencies equal to those of these waves.

(iii) At lower values of R_δ the main effect of diffusion is stabilizing or smoothing, as expected. However, a stronger diffusive effect is necessary to remove the instability (see (i)) of layers with vorticity maxima, which is large and almost independent of R_δ, than to remove the weaker instability (see (ii)) of layers with monotonic vorticity. Accordingly, the 'critical' R_δ (separating values of R_δ at which waves of some lengths are unstable from those at which none are) is lowest for layers with pronounced vorticity maxima; it increases as the vorticity maximum approaches the wall, to take considerably higher values for layers with monotonic vorticity, and continues to rise as the vorticity gradient becomes more precipitous (Schlichting 1940, 1955; Pretsch 1941*b*; Lin 1955).

(iv) Although the above theory is for two-dimensional vortex layers, it can be applied to three-dimensional boundary layers if one considers separately the stability of the 'cross-stream' and 'streamwise' vorticity distributions (Section 2.8). Now, since the total streamwise vorticity (integrated across the layer) is zero, it must have a maximum somewhere. It may happen, therefore, if the external flow is accelerating, that R_δ has a value for which the cross-stream vorticity is stable but the streamwise vorticity unstable, leading to concentration of the latter vorticity in 'streaks' which may be visible on oilflow photographs (Gregory, Stuart, and Walker 1955).

The implications of these four results in the problem of transition to turbulence are discussed in Section 3.2. Meanwhile, some explanatory remarks which help to throw light on the essential facts (i) and (ii) are offered, although any attempt at a complete explanation that omits the mathematical theory is out of the question.

The comparison in Fig. II. 17 of a boundary layer in accelerated flow (*a*) and one in retarded flow (*b*) is at first sight relevant to (i). In (*a*), the slight additional vorticity at P (to whose effect must be added that of its image P') produces 'downwash' ahead, whose convective effect on the undisturbed vorticity distribution (which decreases upwards) is to reduce the vorticity in that region, whither the vortex is moving. This fact appears to give the process positive stiffness; the same is true in (*b*) of a vortex at Q. However, the downwash ahead of the vortex at R convects *increased* vorticity into the region whither it is moving, since the undisturbed vorticity increases upwards. This might be taken to signify negative stiffness, and consequent amplification of disturbances, in (*b*) but not in (*a*).

However, such a conclusion would prove too much, indicating instability also for flows in which the vorticity increases upwards, not to a maximum in the layer, but monotonically until a second wall is reached. Furthermore, any simple mathematical model of a convection process of the kind just described, if it takes into account the fact that the convective increase of vorticity ahead of the vortex is balanced by an equal and opposite decrease behind it, shows that the result is merely to augment the effective *velocity* of convection of the disturbance R (while reducing those of P and Q), without introducing any amplification.

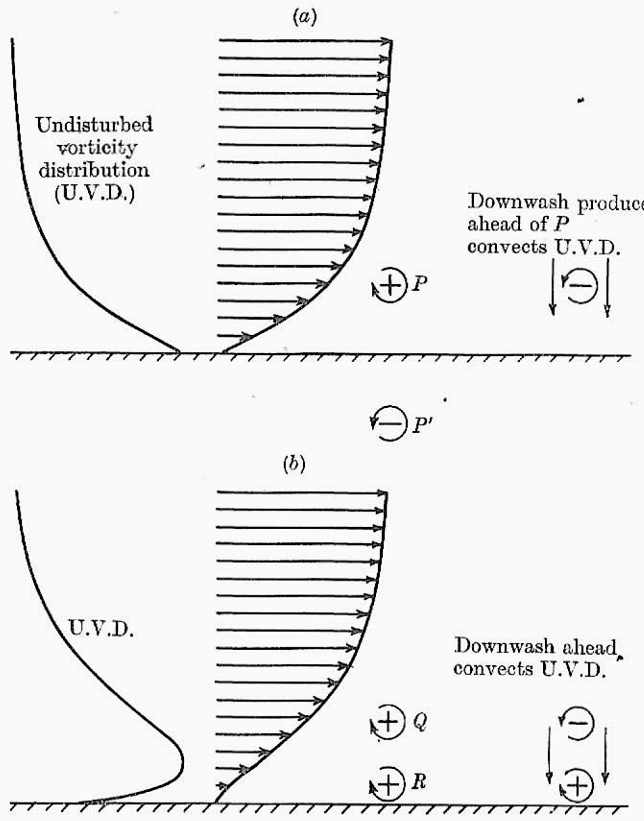

FIG. II. 17. Convective effect of additional vorticity on the undisturbed vorticity distribution, for layers with (*a*) monotonic vorticity, (*b*) a vorticity maximum in the midst of the layer.

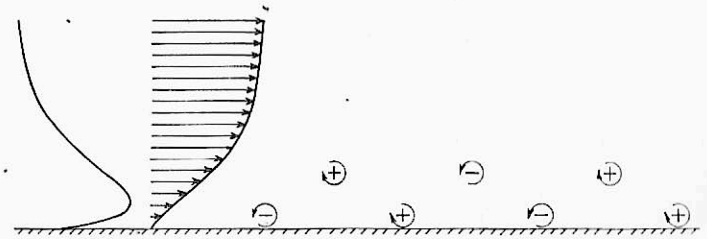

FIG. II. 18. Schematic representation of disturbance to which a layer with a vorticity maximum is unstable.

A mechanism of instability closer to the true one indicated by the mathematical theory is illustrated in Fig. II. 18, where two disturbances are shown, the one above the vorticity maximum having a phase lead over the one below. The possibility of some wave of this general form

receiving amplification as it travels along is strongly indicated by two facts: first, that every vortex shown produces such vertical convection of the undisturbed vorticity distribution as tends to augment the disturbances at *both* adjacent vortices; and, secondly, that the above-mentioned increase in the velocity of convection for the lower vortices, and decrease for the upper ones, helps to 'keep them in step'. Together, these facts amount to a physical explanation of the destabilizing effect of the vorticity maximum.

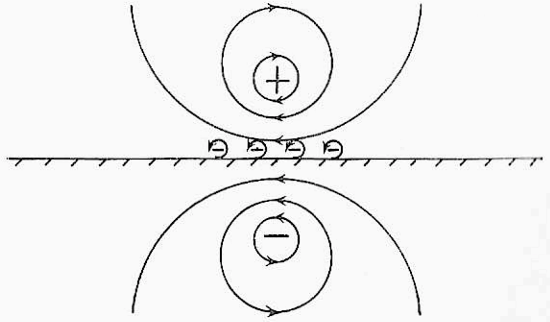

FIG. II. 19. Illustrating how vorticity near the wall causes the generation of vorticity of opposite sign at the wall.

Passing to (ii), all authorities are agreed (see, for example, Lin 1945, p. 291, Taylor 1915, and Lin 1954*b*) that the destabilizing effect of viscosity for certain wavelengths operates in the region very close to the wall. In other words, it results from the diffusion, away from the wall, of vorticity produced there in accordance with the mechanism of Section 1.7. Indeed, Fig. II. 19 shows that additional vorticity of positive sign near the wall causes vorticity of negative sign to be generated at the wall, which for waves of appropriate length must diffuse out as far as the original vortex in time to reinforce the negative phase of the wave when it arrives.

However, the total effect of even a very small amount of diffusion is certainly more complicated than this. The inviscid disturbance theory for boundary layers in accelerating flow is exceptional, in that general disturbances do not show normal longitudinal dispersion into wave packets, each with its own phase velocity and group velocity; rather, a wave system tends to get set up, in which disturbances at every distance from the wall have a phase velocity equal to the local undisturbed velocity. (This possibility corresponds in the mathematical theory to the pole of the vorticity at the 'critical' speed.) Clearly, the resulting interference of waves will be greatly reduced by even the

smallest amount of diffusion. These considerations contribute to the complication of the theory from which the result (ii) is finally derived. All the theories are more fully discussed in Chapter IX, together with material on the stability of internal flows, etc.; see also Schlichting (1955) and Lin (1955).

3.2. *Transition to turbulence*

Despite the advance of stability theory, and parallel advances in theoretical and observational knowledge of turbulent flows, the intervening topic, namely the transition between slightly disturbed laminar flow and fully turbulent flow, remains one of the least understood parts of aerodynamics.

Two opposing factors combine to make the value of R_δ at which a vortex layer becomes fully turbulent different from the 'critical' R_δ (Section 3.1) at which instability first appears. The first is that a layer which is stable to small disturbances can be unstable to larger ones. This is well attested for all types of flow, internal and external; the value of R_δ for onset of turbulence can normally be reduced by a factor of 5 or more by deliberate introduction of disturbances, such as involve velocity fluctuations around, say, 3 per cent. of the mean. The main physical feature in the growth of such large disturbances, that is absent from the theory for small disturbances, is self-convection of the disturbance-vorticity distribution (as distinct from its convection by the undisturbed flow, or the convection of undisturbed vorticity by the disturbance). A possible way in which self-convection may help a fluctuating vorticity distribution to grow is by changing the mean vorticity distribution so as to make it more unstable (perhaps introducing a maximum in the midst of the layer); other possibilities are discussed in Chapter IX.

The second factor is that R_δ, at least in external aerodynamics, increases with distance in the direction of motion. Now, under 'smooth' conditions (of low mainstream turbulence, vibration, roughness, etc.), disturbances may be expected to follow the stability theory at least initially, and this has been verified experimentally in certain cases (Schubauer and Skramstad 1947). In particular, they have a certain rate of amplification with time, but also are convected downstream (more precisely, they travel at the appropriate group velocity, with a a certain degree of dispersion, which causes a localized disturbance to grow in size). As they become amplified, the effect of self-convection may increase the amplification rate, at least at first; but disturbances

must have reached regions where R_δ is substantially greater than its critical value before they attain the 'equilibrium' turbulence level (Section 3.3).

There is then some further delay before different localized disturbances have grown to fill the whole flow. This occurs in a 'transition region', which in the much studied boundary layer with uniform external flow is from a quarter to a half as long as the distance of its front from the leading edge. It is filled with a random collection of 'turbulent spots', which grow as they move downstream until spots all over the surface have merged into one turbulent boundary layer (Emmons 1951, Schubauer and Klebanoff 1955, Hama, Long, and Hegarty 1957, Dhawan and Narasimha 1958). The velocity variation at a point is found, by hot-wire measurements (Chapter X), to be almost steady at its laminar-flow value, except during intermittent 'bursts' of large, turbulent fluctuations, during which all characteristics of the record, including mean velocity, are as in a fully turbulent boundary layer. An interesting feature of the spots or bursts is their 'sharp front'. Like the simpler self-convection processes which can give a sharp front (the 'shock wave') to high-frequency acoustic pulses, the self-convection of turbulent vorticity shows a tendency (only partially understood) to steepen the vorticity gradient at the edge of a patch of turbulence; this tendency prevents its weakening by diffusion, and is responsible also for the sharpness of image of bullet wakes in spark photographs, such as Fig. II. 20 (Plate). As the fraction of time occupied by these bursts increases from 0 to 1 through the transition region, all averaged properties (including skin friction, see Section 3.3) adjust proportionately, from laminar-layer to turbulent-layer values.

Under 'smooth' conditions, it has been found that transition does not normally begin before a point, at which small disturbances, of at least some frequencies, should have been amplified by a factor of order 10^4, according to calculations (Smith 1956*a*) which allow for the variation of amplification rate as the disturbance passes through parts of the boundary layer with different undisturbed-vorticity distributions, but ignore its dependence on amplitude. On the other hand, a much smaller factor would suffice in rough conditions.

For example, in a layer with uniform external flow, the critical R_{δ_1} (based on displacement thickness) is 420, which gives 6×10^4 for R_x (based on the distance x from the point of attachment). But the value of R_{δ_1} at the beginning of transition is around 3,000 under smooth conditions (giving $R_x = 3\times10^6$), and it falls away as the degree of

disturbance increases, to a minimum around $R_{\delta_1} = 500$ (giving $R_x = 8 \times 10^4$); in this very 'rough' flow, the 'two factors' which were discussed above almost cancel.

If, however, the boundary layer passes into a region of retarded flow, the critical R_{δ_1} quickly falls (say, to around 100), while δ_1 rapidly increases (Section 2.4); this may jerk a laminar boundary layer into turbulence, well before it would have separated, and thus help it, as we shall see, to avoid separation altogether. On the other hand, in the region of accelerating flow near the front stagnation point, the critical R_{δ_1} is around 10^4, while the layer is thin, and transition occurs in this region only at values of R_x exceeding 10^8. Then, as the external-flow gradient U' falls, so does the critical R_{δ_1}, while δ_1 increases, and transition becomes steadily more likely.

Although the above remarks about this difficult subject are based largely on data for two-dimensional boundary layers, they are believed to have substantial general value, except in that, for three-dimensional flows, the instability of the streamwise vorticity distribution (Section 3.1) is an important additional source of transition.

3.3. *The turbulent boundary layer*

We pass now to a subject where enormous volumes of quantitative information exist, but of which a brief qualitative survey will suffice for the purposes of this volume.

Although the rate of amplification of disturbances to a boundary layer may be initially positive, and even increasing with amplitude, it becomes zero by the time the layer is 'fully turbulent', when the ratio of the root-mean-square fluctuation of velocity to the external flow velocity has a maximum of around 10 per cent. (attained, as we shall see, very close to the wall) and shows no further tendency to increase.

One reason for this change is that turbulence redistributes the vorticity in such a way that viscous diffusion becomes more effective in countering the amplification of the disturbances. Especially, it concentrates most of the vorticity much closer to the wall than before, although at the same time allowing some straggling vorticity to wander away from it farther. Fig. II. 21 (derived principally from Schubauer and Klebanoff 1955) shows the vorticity distribution in a two-dimensional laminar layer with uniform external flow, where transition begins, at $R_x = 2{\cdot}3 \times 10^6$, and also the distribution of the mean vorticity $\bar{\omega}$, and of the root-mean-square fluctuation of vorticity $\sigma\{\omega\} = \{\overline{(\omega - \bar{\omega})^2}\}^{\frac{1}{2}}$, in the fully turbulent layer at the rear of the transition region, where

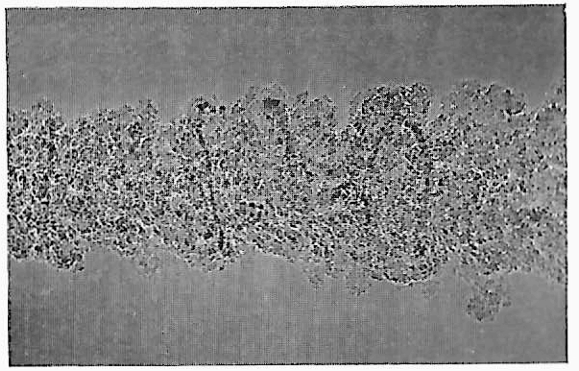

FIG. II. 20. Spark photograph of the wake of a bullet. (Ballistics Research Laboratory, Aberdeen Proving Ground, 1958)

$R_x = 3{\cdot}3 \times 10^6$. During transition some 95 per cent. of the vorticity has moved closer to the wall, much of it very close indeed; the mean vorticity at the wall, $\bar{\omega}_w$ (which is τ_w/μ, where τ_w is the skin friction), has risen to 8 times the laminar value, and $\bar{\omega}$ now falls precipitously away from this maximum. However, the other 5 per cent. of the mean vorticity has moved out much farther than it would have in the normal development of the laminar layer.

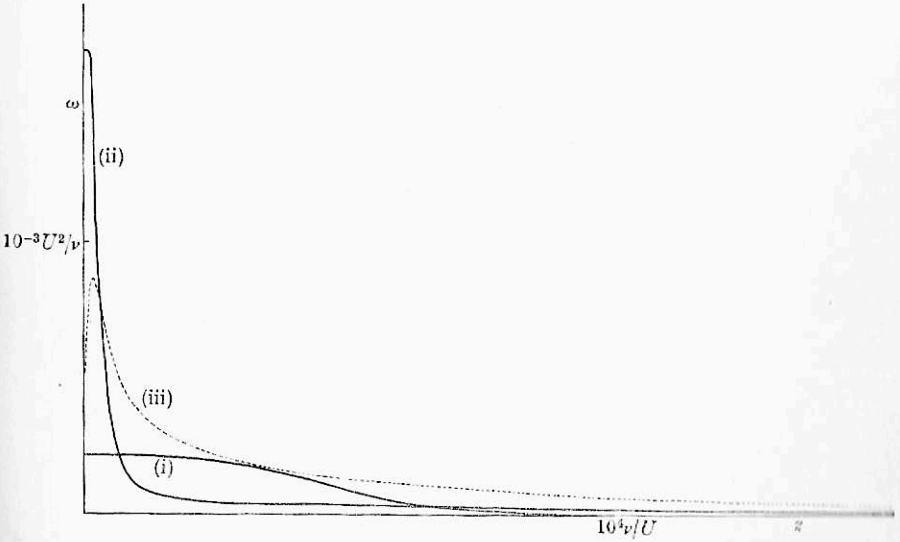

FIG. II. 21. Distribution of mean vorticity in a boundary layer with uniform external flow; (i) at beginning, (ii) at end, of transition. Curve (iii) gives rough values of the root-mean-square fluctuation $\sigma(\omega)$ at the end of transition.

Downstream, the turbulent boundary layer grows principally by extension of this 'tail' of the vorticity distribution (a typical angle between the edge of the boundary layer and the surface being 1°). By contrast, the mechanism concentrating vorticity close to the wall (which is discussed below) permits that concentration to fall off only very gradually indeed—much more gradually than the boundary-layer thickness increases. Nevertheless, small quantities of vorticity do continually break loose from the region of concentration; and the fluctuations in w (velocity component normal to the surface) which they themselves induce have a statistical tendency to spread that vorticity over a greater and greater area. At any one instant the region of vorticity has an irregular edge, like that of the wake photograph Fig. II. 20 (Plate). The turbulence is measurably intermittent in the outer half of the

boundary layer (Dhawan and Narasimha 1958), because the induced velocity fluctuations in the irrotational-flow regions between protruding tongues of vorticity are relatively mild. By contrast, the 'busy' motion at the edges of those tongues (visible clearly in, say, a smoke jet) is continually forming convolutions which 'entrain' irrotational fluid into the region of vorticity, where diffusion quickly makes it rotational.

This mechanism for spreading out the vorticity in, say, the outer four-fifths of a boundary layer (or in the whole of a 'free' turbulent layer, such as a wake) is analogous to the statistical mechanism of diffusion (Section I. 3), except that the random motion is of lumps of vorticity instead of individual molecules. It is commonly referred to as 'turbulent diffusion', and it has been shown that the resulting distributions of mean vorticity and mean velocity in the regions in question behave as if the diffusivity ν (of vorticity or momentum) were increased by the presence of turbulent diffusion to a much higher value ν_T (Townsend 1956). For the turbulent layer of Fig. II. 21, ν_T/ν is about 40, but it increases with the Reynolds number R_δ based on layer thickness. For a wake far behind a cylinder of drag D per unit length, ν_T is about $0{\cdot}02\,D/\rho U_\infty$. There is evidence in both cases that the effective ν_T falls off in the region of markedly intermittent turbulence.

This statistically uniform churning-up of the outer four-fifths of a boundary layer, by vorticity which has escaped from the region of concentration, is both regulated as regards intensity, and also prevented from acting unchanged in the inner fifth, by a mechanism depending crucially on the presence of the solid surface, although assisted in its operation by the outer vorticity fluctuations.

The main effect of a solid surface on turbulent vorticity close to it is to *correlate inflow towards the surface with lateral stretching*. Note that only the stretching of vortex lines can explain how during transition the mean wall vorticity increases as illustrated in Fig. II. 21; and only a tendency, for vortex lines to stretch as they approach the surface and relax as they move away from it, can explain how the gradient of mean vorticity illustrated in Fig. II. 21 is maintained in spite of viscous diffusion down it—to say nothing of any possible 'turbulent diffusion' down it, which the old 'vorticity transfer' theory supposed should occur. It is relevant to both these points that Fig. II. 21 relates to uniform external flow, which implies zero mean rate of production of vorticity at the surface; but, even in an accelerating flow, the rate of production UU' is too small to explain either.

A simplified illustration of how inflow towards a wall tends to go

with lateral stretching, and outflow with lateral compression, is given in Fig. II. 22. Doubtless some longitudinal deformation is usually also present, which reduces the need for lateral deformation (perhaps, on the average, by half). However, there is evidence (from attempts to relate different types of theoretical model of a turbulent boundary layer to observations by hot-wire techniques; see, for example, Townsend

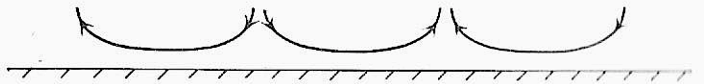

FIG. II. 22. Correlation of inflow with lateral stretching, and outflow with lateral compression, of vortex lines (the mean flow is normal to the plane of the paper).

1956) that the larger-scale motions (which push out the 'tongues' of rotational fluid discussed above) are elongated in the stream direction, as if their vortex lines had been stretched longitudinally by the mean shear; in such motions, the correlation between inflow and lateral stretching illustrated in Fig. II. 22 would be particularly strong. We may think of them as constantly bringing the major part of the vorticity in the layer close to the wall, while intensifying it by stretching, and, doubtless, generating new vorticity at the surface; meanwhile, they relax the vortex lines which they permit to wander into the outer layer. Smaller-scale movements take over from these to bring vorticity still closer to the wall, and so on. Thus, the 'cascade process', which in free turbulence (see, for example, Batchelor 1953) continually passes the energy of fluctuations down to modes of shorter and shorter length-scale—because at high Reynolds numbers motions in a whole range of scales may be unstable, which implies that motions of smaller scale can extract energy from them—this cascade process has the additional effect in a turbulent boundary layer of bringing the fluctuations into closer and closer contact with the wall, while their vortex lines are more and more stretched.

Ultimately, they reach a region where gradients have become so intense that viscous diffusion counteracts the effect of further stretching. A measure, η, of the thickness of the 'viscous sub-layer', where owing to diffusion the mean vorticity has reached a uniform value (which is $\bar{\omega}_w$), is obtained by balancing rates of diffusion, of order $\nu\bar{\omega}_w/\eta$, and of convection, of order $(\bar{\omega}_w\,\eta)\bar{\omega}_w$, to give

$$\eta = (\nu/\bar{\omega}_w)^{\frac{1}{2}} = \nu(\tau_w/\rho)^{-\frac{1}{2}}. \tag{32}$$

Experimentally, uniformity of $\bar{\omega}$ extends to about $z = 5\eta$ (Townsend

1956; but this is *not* a 'laminar' sub-layer, as supposed in the early literature; the root-mean-square fluctuation of ω is about 30 per cent. of the mean). On the other hand, viscous diffusion ceases to be important compared with convection effects for $z > 30\eta$. We should note the extremely small value of η, as appears from the order of magnitude, 30, of the Reynolds number $U\eta/\nu$.

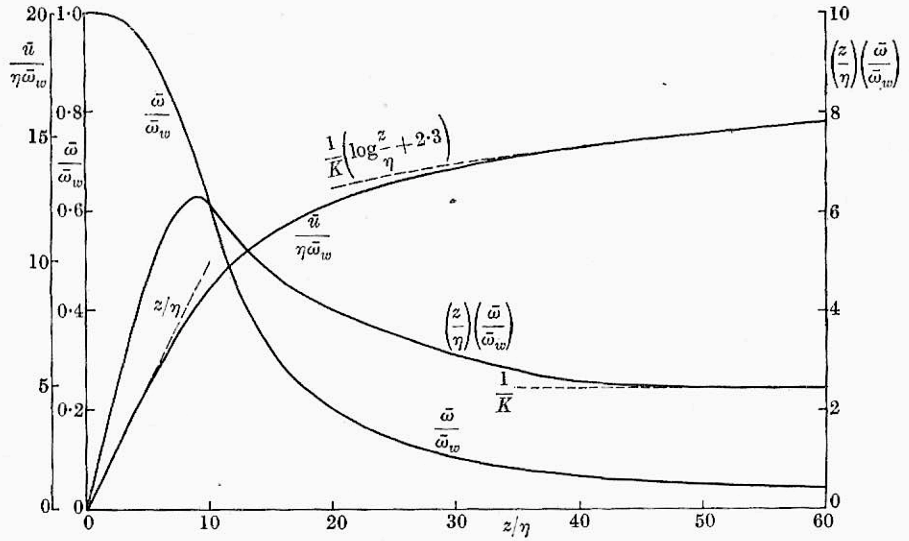

FIG. II. 23. The law of the wall (mean values). A plot of $\bar{\omega}/\bar{\omega}_w$, $(z/\eta)(\bar{\omega}/\bar{\omega}_w)$, and $\bar{u}/\bar{\omega}_w\eta$ against z/η in the equilibrium layer near a solid surface (Laufer 1954).

Experiments on a wide range of turbulent flows (including flow in pipes) have shown that a layer adjacent to the solid surface, of thickness far greater than η, and nearer to a tenth of the thickness of the whole region of vorticity, is approximately identical in structure (statistically speaking) in all such flows, differing only in intensity, as measured, say, by $\bar{\omega}_w$. The violent agitations of such an inner layer maintain its 'equilibrium' of structure, although the fluid in it may have come from a region where $\bar{\omega}_w$ was different, because the downstream convection process is slow by comparison. It follows by dimensional analysis (Section I. 5) that any quantity in this region, when multiplied by a combination of $\bar{\omega}_w$ and the constants ρ and μ to make it non-dimensional, is a function of z/η alone (the 'law of the wall'). This functional relationship, for various means and standard deviations of observed quantities, is given in Figs. II. 23 and 24. The simplifications for $z/\eta > 30$ may be ascribed to the unimportance of viscous diffusion in this region, where the transport of momentum towards the surface, at a rate τ_w

per unit area, to make up for the momentum removed there by skin friction, takes place solely by turbulent convection. In this region, $\bar{\omega}$, for example, depends on τ_w, ρ, and z alone, giving

$$\bar{\omega} = \frac{(\tau_w/\rho)^{\frac{1}{2}}}{Kz} = \frac{\bar{\omega}_w\eta}{Kz}, \tag{33}$$

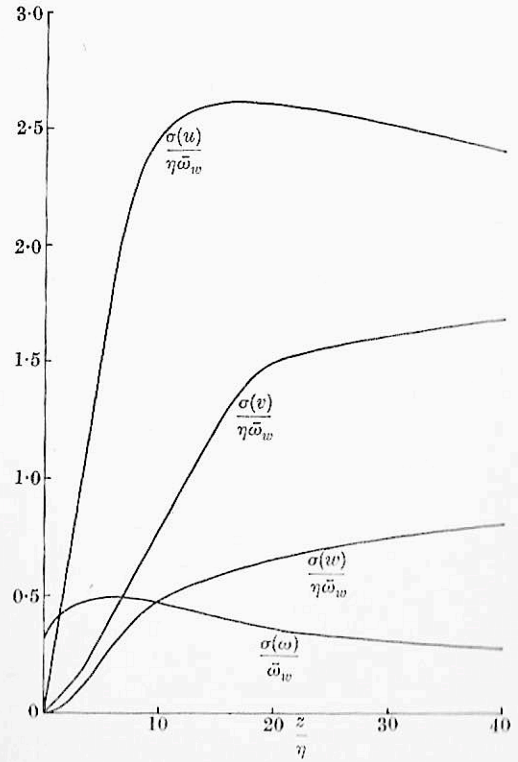

FIG. II. 24. The law of the wall (approximate root-mean-square fluctuations). A plot of $\sigma(\omega)/\bar{\omega}_w$, $\sigma(u)/\bar{\omega}_w\eta$, $\sigma(v)/\bar{\omega}_w\eta$, $\sigma(w)/\bar{\omega}_w\eta$ against z/η in the equilibrium layer.

where K is a constant determined experimentally as $0{\cdot}40 \pm 0{\cdot}01$. Integrating,

$$\bar{u} = \frac{(\tau_w/\rho)^{\frac{1}{2}}}{K}\left\{\log\frac{z}{\eta} + A\right\}, \tag{34}$$

where A is a constant determined experimentally as $2{\cdot}5 \pm 0{\cdot}2$ (Coles 1955). Equations (33) and (34) hold if z exceeds 30η and is less than about a tenth of δ.

It would be out of place here to discuss further details of the inner and outer layers and the interaction between them. We must note, though, how the turbulent layer reacts to removal of vorticity at the

wall. Because of the mechanism, which continually concentrates vorticity at the wall, a much more extensive region of negative vorticity-source strength UU' at the surface is required to reduce $\bar{\omega}_w$ to zero than for the laminar layer, a typical required reduction in U being not 5 per cent. but 30 per cent. This is why transition to turbulence may so greatly delay, or even prevent, separation.

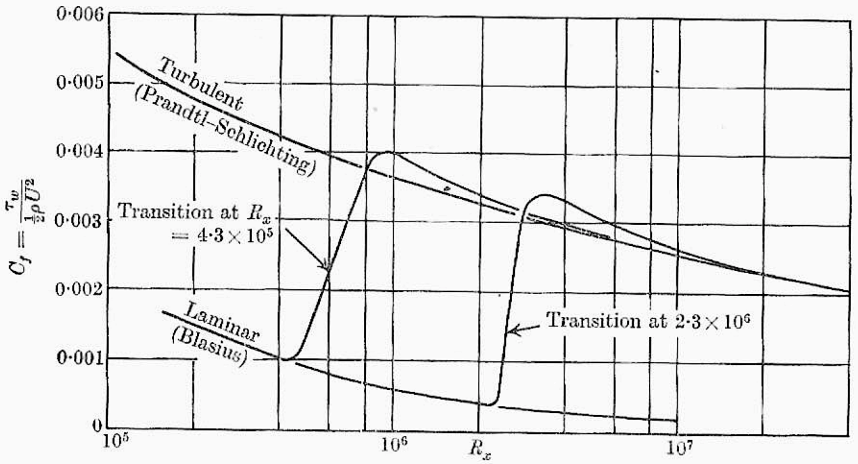

FIG. II. 25. The local skin-friction coefficient C_f plotted against R_x for boundary layers on smooth surfaces with uniform external flow and different values of R_x at transition.

We illustrate also, in Fig. II. 25, the variation of the skin-friction coefficient,

$$C_f = \tau_w/(\tfrac{1}{2}\rho U^2), \tag{35}$$

for uniform external flow over a smooth surface with various values of R_x at transition (Dhawan and Narasimha 1958). These graphs have general illustrative utility, since for the reasons just given τ_w depends less strongly on the distribution of U with x than in a laminar layer. For rough surfaces, the gradual change in C_f, as R_x increases, flattens out to a constant value where the Reynolds number of the flow over a typical roughness element becomes large enough for it to shed a turbulent wake; in the case of a very rough surface, a rather abrupt *rise*, to a value as high as 0·01, may precede this flattening (Goldstein 1938, p. 380).

4. Variation of flow patterns with Reynolds number

4.1. *Flow around bluff bodies*

To illustrate how knowledge of the properties of vorticity, boundary layers, and turbulence is applied, we end this chapter with some

remarks on the variation of the flow pattern with Reynolds number,

$$R = \rho U_\infty l/\mu = U_\infty l/\nu, \tag{36}$$

for the steady flow about a stationary body of length-scale l, and given shape and attitude, under conditions when ρ and μ can be regarded as constant; such flow patterns were shown in Section I. 5.1 to depend on R alone. First, we consider 'bluff bodies', which include most shapes not specifically 'streamlined' for good aerodynamic performance, and which may be defined as those for which 'thin-wake' flow is impossible, however far forward the boundary layer may increase its resistance to separation by transition to turbulence.

When R is very small indeed (say, $R < 1$) a type of flow very different from those discussed earlier in this chapter occurs (see Chapter IV). This is because convection of vorticity is slow, compared even with diffusion over distances of order l. It follows that, in the outer regions of vorticity, convection proceeds at almost the uniform speed U_∞, which, balanced against a speed of order ν/s for diffusion through distance s, gives ν/U_∞ as a measure of the upstream penetration of vorticity, instead of the $\sqrt{(\nu l/U_\infty)}$ for large R which follows from the use of (14). Actually, diffusion makes the vorticity fill an enormous paraboloid of revolution, with focus in the body and vertex a distance of 2 or 3 times ν/U_∞ upstream of it.

Near the body, on the other hand, the scale of the vorticity variations is l, and hence diffusive flow is large compared with convective flow. Accordingly, the separation mechanism, whereby (Section 2.4) convection continually alters the vorticity distribution so as to call for generation, over parts of the surface, of vorticity in the opposite sense, fails to operate; on the contrary, as vorticity diffuses away from the body, its effect in maintaining the no-slip condition at the surface is weakened, requiring the generation of more vorticity in the same sense. Therefore, separation does not occur, or, more precisely, is delayed until a final 'nodal point' at the rear of the body.

In this type of flow, which is treated in detail in Chapter IV, viscous stresses near the body are of order $\mu U_\infty/l$, as also are dynamic pressures, since the usual terms of order ρU_∞^2, needed to make dynamic pressure gradients balance changes of momentum, are small compared with terms of order $\mu U_\infty/l$, needed to make them balance gradients of viscous stress. It follows that the drag is of order $\mu U_\infty l$ for very small R, so that the coefficient C_D (Section I. 5.2) satisfies

$$C_D \sim A/R \quad \text{as} \quad R \to 0, \tag{37}$$

where A is a constant, which is 24 for a sphere of diameter l if its projected area $\frac{1}{4}\pi l^2$ is used in the definition of C_D, equation (I. 44).

Similar arguments hold for two-dimensional flow about an infinite cylinder, but the functional dependence of C_D on R as $R \to 0$ is slightly different, because diffusion at a steady rate from an infinite cylinder makes that which diffuses grow logarithmically with distance from the cylinder, instead of becoming constant; it follows that a distribution of vorticity diffusing to a distance of order ν/U_∞, and producing a total change U_∞ in velocity, must involve changes of order $U_\infty/\log(\nu/U_\infty l)$ over distances of order l. This alters the previous argument, introducing a $\log(R^{-1})$ factor in the denominator of C_D, as in the formula

$$C_D \sim 8\pi/R\log(7{\cdot}4R^{-1}) \quad \text{as } R \to 0$$

for a circular cylinder of diameter l.

In the region between $R = 1$ and $R = 10$, convection of vorticity near the body begins to assume the role described in Section 2, leading to the formation of a separation line, which moves forward from the rear as R increases above a value R_s in this range. The flow then has a separation bubble and a steady laminar wake, provided that R remains below the value R_l at which the wake becomes unstable. Fig. II. 26 (Plate) illustrates three flows of this kind for the circular cylinder, with $R = 3{\cdot}9$ (which is near R_s), $R = 18{\cdot}6$, and $R = 33{\cdot}5$. The last value is large enough for the arguments of boundary-layer theory to have real value; thus, the displacement thickness at the first point of attachment is only 0·11 radii.

It is still not known for certain what determines the length of the separation bubble, or whether this would continue to grow with increasing R if the flow did not become unstable above $R = R_l$, which is about 40 for the circular cylinder. Batchelor (1956) argues that l_s/l (where l_s is the length of the separation bubble) would tend to a constant with increasing R, while C_D would tend to zero; but Imai (1957*a*) argues that l_s/l would increase in proportion to R, while C_D would tend to the value given by the Helmholtz–Kirchhoff discontinuous flow theory.

The mode of redistribution of vorticity which builds up to large amplitude in the wakes of cylinders at Reynolds numbers just above R_l is of the general type illustrated in Fig. II. 18, leading to the staggered parallel rows of vortices known as Kármán's vortex street. Behind a circular cylinder, a regular street like that illustrated in Fig. II. 28 (Plate) occurs for Reynolds numbers between $R_l = 40$ and around 200. Fig. II. 27 (Plate) shows its build-up for five Reynolds numbers

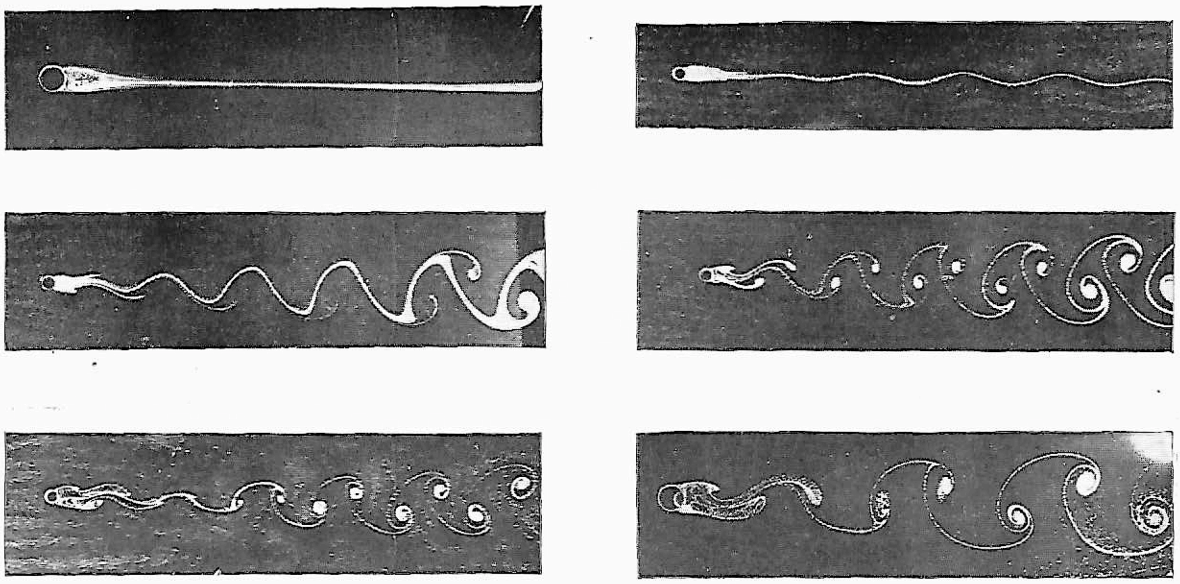

FIG. II. 27. Flow about a circular cylinder at $R = 31{\cdot}6$, $54{\cdot}8$, $65{\cdot}2$, 73, $101{\cdot}5$, 161.
(Homann 1936*a*)

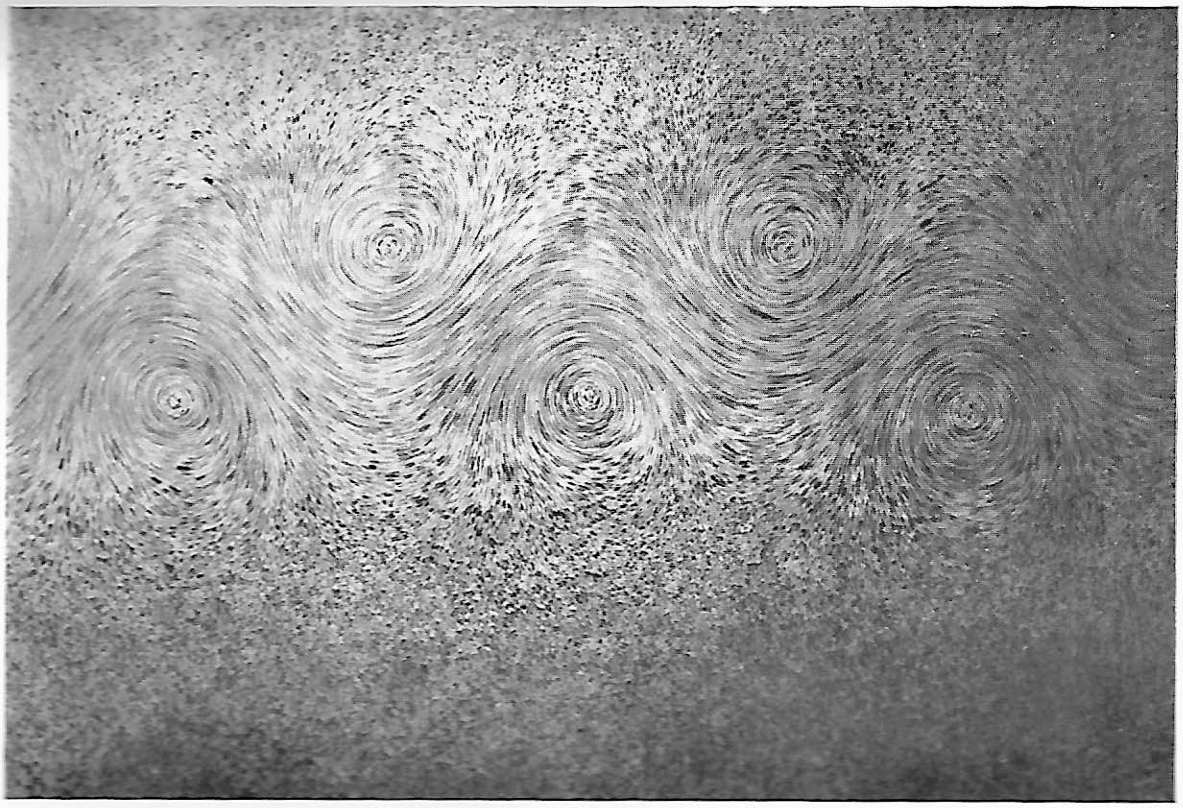

FIG. II. 28. Kármán vortex street behind a cylinder. (Richards 1933)

in this range, the lowest ($R = 54{\cdot}8$) being near to the (somewhat increased) value of R_t appropriate to the tunnel width that was used. As R increases still more, other modes become capable of amplification, which, together with the 'cascade process' (Section 3.3), namely the break-up of larger eddies by instability into smaller ones, produces a more and more irregularly turbulent wake. When the vorticity close to the cylinder is fluctuating between large positive and negative values, there is a substantial fluctuating lift on the cylinder (compare Section 2.5), and the equal and opposite reaction on the air generates the sound known as Aeolian tones (Phillips 1956).

There is less information on three-dimensional bluff bodies, such as spheres, in this range of Reynolds numbers, but values of R_t appear to be higher, about 500 for spheres (Schmiedel 1928, Möller 1938), because no mode of vorticity redistribution in their wakes has the very marked instability of rows of staggered parallel vortices. The dominant mode is often a spiral vortex. Similarly, R_s is greater (around 17) for spheres (Jenson 1959).

The configuration of mean streamlines (curves to which the mean of the velocity vector is everywhere tangential) in the turbulent region immediately behind any bluff body is often similar to what it would be in laminar flow with ν increased to a greater value, the 'eddy viscosity' ν_T (compare Section 3.3). The 'effective Reynolds number' $U_\infty d/\nu_T$, based on eddy viscosity, is commonly between 40 and 50 for cylinders (Imai 1957*a*). Accordingly, the part of C_D due to surface pressures, which depends largely on this mean-streamline pattern, remains approximately constant from $R = R_t$ up to the value $R = R_c$ (of order 10^5) at which boundary-layer transition begins to affect the separation point. At the same time, the part of C_D due to skin friction falls in proportion to $R^{-\frac{1}{2}}$, since the viscous stresses which produce it are of order $\mu U_\infty/\delta$, which in turn is of order $\rho U_\infty^2 R^{-\frac{1}{2}}$ because the boundary-layer thickness δ is of order $(\nu l/U_\infty)^{\frac{1}{2}}$. Fig. II. 29 illustrates these effects for a circular cylinder. For a sphere, the two parts of C_D have not been separately measured, but the variation of C_D with R (Fig. II. 30) is consistent with a pressure contribution of around 0·4 and a skin-friction contribution of around $7R^{-\frac{1}{2}}$ (compare 1·0 and $4R^{-\frac{1}{2}}$ for the circular cylinder).

For both shapes there is a striking fall in C_D when R passes through the critical value R_c (defined conventionally for the sphere as the value for which $C_D = 0{\cdot}3$). At $R = R_c$, transition in the boundary layer begins to precede separation, and therefore to postpone it (Section 3.3).

The fall in C_D, due to the resulting narrowing of the wake region of fluid disturbed by the body, is not quite abrupt because of the intermittent character of transition (Section 3.2).

The fact that R_c depends, not only on body shape, but also on less obvious features, such as roughness and the level of turbulence in the wind-tunnel, an increase in either of which tends to reduce R_c (Section

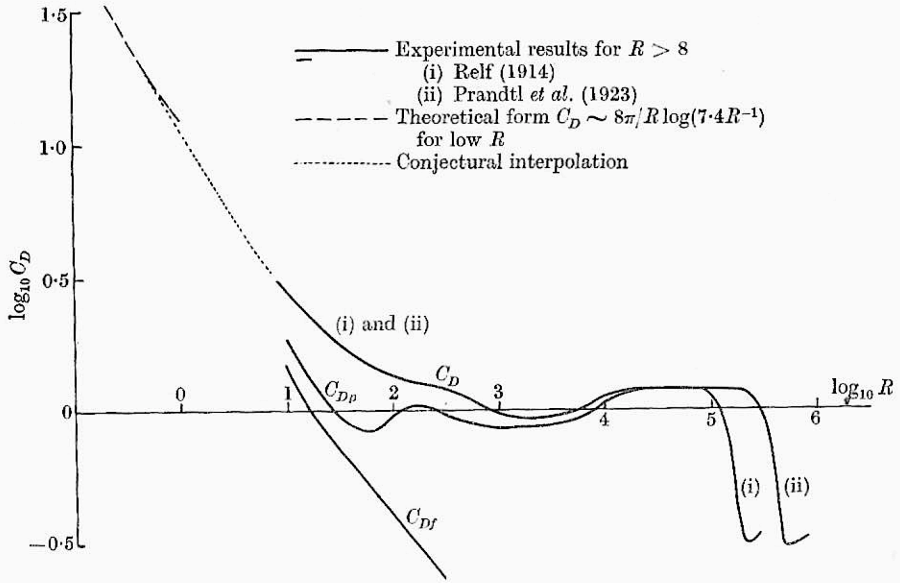

FIG. II. 29. Drag coefficient C_D as a function of R for flow about a circular cylinder, with the separate contributions (obtained by Thom 1928) C_{Dp} (due to normal pressure) and C_{Df} (due to skin friction).

3.2), means that, near $R = 10^5$, such non-dimensional coefficients as C_D are not unique functions of R for a given shape (Figs. II. 29 and 30). This illustrates well (compare Section I. 5.5) the dangers of too simple-minded an approach to dimensional analysis; one might assume from the smallness of non-dimensional parameters formed from the roughness height ϵ, or the root-mean-square velocity fluctuation u' of the undisturbed stream, that these would not affect the flow pattern, but the experimental failure of the resulting similarity law near $R = 10^5$ tells us that in this region such factors do play a part.

Subcritical and supercritical distributions of pressure around a sphere are plotted in Fig. II. 31. The supercritical distribution is close to the theoretical distribution for irrotational flow up to the separation point ($\theta = 140°$); the slight inflexion in the curve is due to the sudden drop in displacement thickness on transition, as vorticity moves in towards

the wall (Section 3.2); while, beyond the separation point, we have locally almost hydrostatic conditions. By contrast, the earlier separation in subcritical flow raises the pressure even upstream of it. As R increases beyond R_c the extent of the turbulent boundary layer increases, and there is some resulting rise in C_D (Figs. II. 29 and 30).

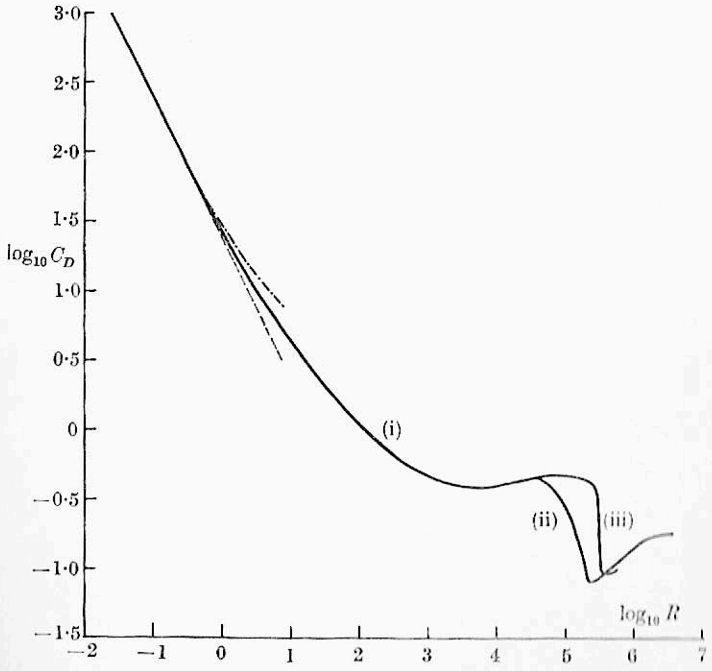

FIG. II. 30. Drag coefficient C_D as a function of R for flow about a sphere. Different observers agree closely on curve (i), but around $R = 10^5$ there are many variations of which curves (ii) (Jacobs and Abbott 1932) and (iii) (Millikan and Klein 1933) represent extremes. The broken line represents the theoretical expression $C_D = 24/R$ for small R. For the dash-dotted line, representing Oseen's theoretical value $C_D = (24/R)(1 + \frac{3}{16}R)$, see Chapter IV.

Prandtl's photographs (Fig. II. 32 (Plate)) of two flows past a sphere, at a Reynolds number which the 'trip wire', present only in the second case, suffices to make supercritical, show the delay in separation and reduction in breadth of wake that boundary-layer transition produces. 'Seam bowlers' in the game of 'cricket' produce a similar effect on one side of the ball only (the yawed 'seam' acting as a trip wire). A new cricket ball is smooth enough for laminar flow to be achieved even at high speeds like 30 m/sec ($R = 1{\cdot}4 \times 10^5$); the lower pressures (Fig. II. 31), on the side where separation is delayed by the action of the seam, generate a swerving force which at these high speeds can make the

ball difficult to hit. A cunning bowler can achieve this condition late in the ball's flight; for example, A. V. Stephens found in unpublished work that, with the seam at 20° incidence, the lift became far less at slightly higher speeds, when turbulent separation occurred on both sides.

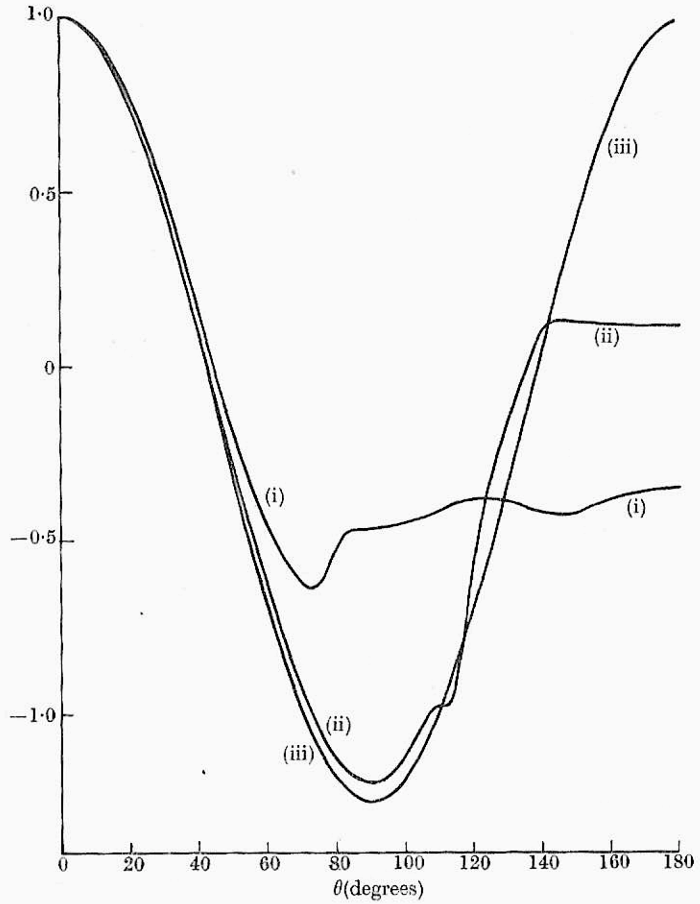

FIG. II. 31. Pressure coefficient $C_p = p_d/(\frac{1}{2}\rho U_\infty^2)$, as function of angular distance θ from front stagnation point, on a sphere in uniform flow: (i) subcritical ($R = 1{\cdot}57 \times 10^5$), (ii) supercritical ($R = 4{\cdot}24 \times 10^5$), (iii) irrotational-flow theory. (Fage 1936*a*.)

Popular opinion, that the effect operates best at high relative humidity, could conceivably have foundation in fact if condensation on to areas of high concave curvature (Section I. 3.2) acts to smooth out roughnesses capable of preventing laminar flow.

Bodies with salient edges often have the line of separation fixed at the edge, at least in most attitudes. This is because flow up to the edge

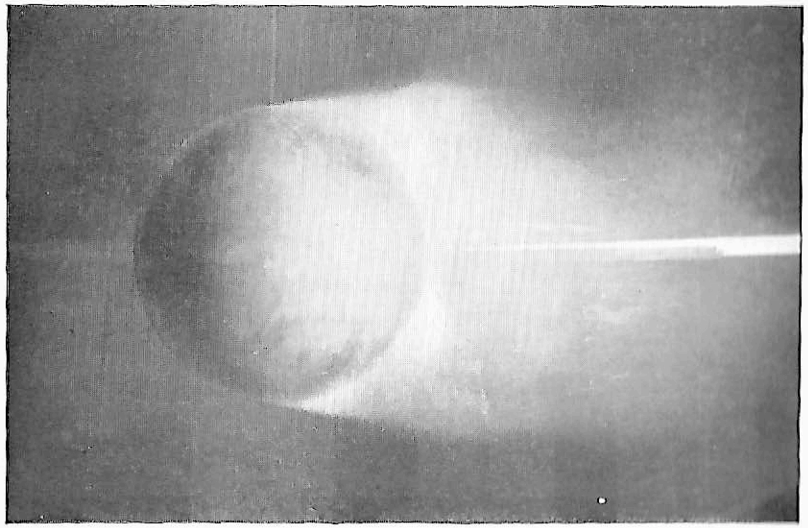

(*a*)

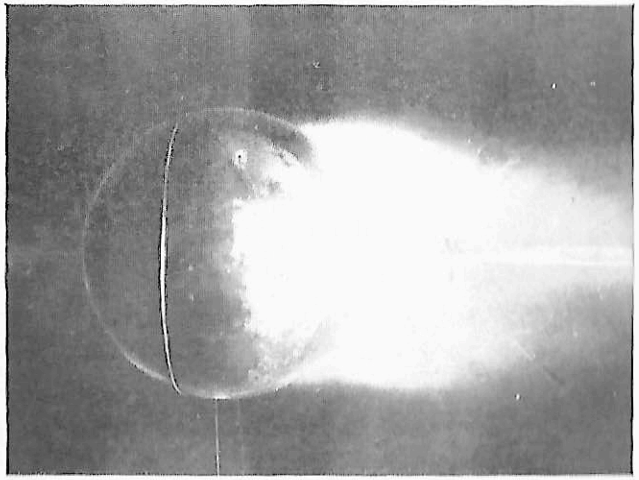

(*b*)

FIG. II. 32. Flow around a sphere (*a*) without, and (*b*) with, a trip wire

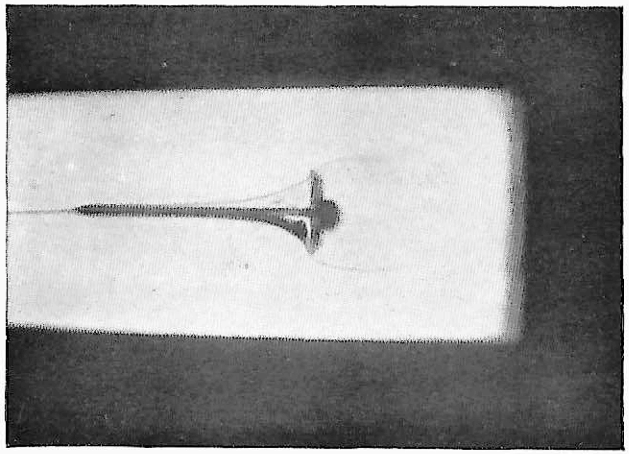

FIG. II. 33. Flow up a step. (Farren 1938)

is accelerating, but flow around it would involve retardations that would separate any boundary layer. For such bodies and attitudes there is no critical Reynolds number; thus, for a long flat strip normal to the stream, C_D (based on the area of the strip) is constant at 2·0 for $R > 1{,}000$.

On the other hand, separation occurs already *ahead* of any corner which is *concave* to the surface, since this would be a stagnation point of an irrotational external flow. Fig. II. 33 (Plate) illustrates the separation bubble produced in the corner for 'flow up a step', with laminar separation; a turbulent boundary layer, on the other hand, yields a shorter bubble because it can support a greater retardation before separating.

4.2. *Flow over streamlined bodies*

Bodies 'streamlined' to achieve thin-wake flow, with the object of reducing C_D to values small compared with 1, will now be discussed at values of R other than those very low ones at which, because separation is not expected in any case, their behaviour differs insignificantly from that of bluff bodies.

As noted in Section 2.5, it is only extremely slender bodies that can avoid separation of a completely laminar layer. One such is a Joukowsky aerofoil of 5 per cent. thickness-chord ratio, which in symmetrical flow has a laminar, unseparated boundary layer up to a Reynolds number R_c (based on the chord c) of around 5×10^6, with C_D around $3{\cdot}6R^{-\frac{1}{2}}$ (Fage, Falkner, and Walker 1929; this exceeds the value $2{\cdot}7R^{-\frac{1}{2}}$ for a flat plate parallel to the stream because of the more rapid thickening of the aerofoil boundary layer in the region of retarded flow). Again, on a suitably designed body of revolution in axisymmetrical flow, an unseparated laminar layer can be achieved above a 'fineness ratio' (length to maximum cross-sectional diameter) of around 7, and the drag is once more slightly above that of a flat plate of the same surface area (Millikan 1932).

As R increases beyond the value at which transition first appears near the trailing edge, the point of transition moves back, but the drag coefficient varies little, because the increase due to the spread of the turbulent layer, and the decrease (like $R^{-\frac{1}{2}}$) in the contribution of the laminar layer (together with a much more gradual decrease in that of the turbulent layer), almost cancel out. Finally, when R is so great that practically the whole layer is turbulent, the drag is almost the same as on a flat plate of the same surface area, since non-uniform external

flow affects turbulent layers only slightly; in particular, it decreases gradually with increasing R (Fig. II. 25).

Surface roughness and mainstream turbulence cause transition to begin at a lower value of R, in which case the level of C_D remains higher during transition. In the fully turbulent régime, roughness also causes the fall in C_D to be arrested at a certain value of R, and C_D then levels out to a constant value, sometimes after a preliminary rise (Section 3.3).

Between these results for extremely slender bodies and those discussed in Section 4.1 for bluff bodies (with C_D a function mainly of the position of separation), there is a fine gradation of intermediate cases; in these, there is some postponement of separation as R passes through a critical interval and transition begins to precede it, but with moderately slender bodies the associated drag reduction may be much smaller than in Section 4.1—say, of the same order as the changes associated with dependence of skin friction on Reynolds number in the interval. In such a case the critical value of R may be not at all obvious from the vagaries of the (C_D, R) curve.

For aerofoils at small angles of incidence α to the oncoming stream, cast-off vorticity leads to a flow 'with circulation' (Section 2.5), in which the external flow velocity takes higher values on the upper surface (so that the pressure is lower there and the aerofoil experiences lift). The boundary layer on this surface is then more prone to separation than that on the lower surface (since the velocity on each must fall to the same value at the trailing edge); but, also, it will become turbulent at a lower Reynolds number R_x based on distance x from the leading edge (and so be helped to resist separation). These two facts lead to complicated variations in the lift coefficient C_L, as well as in C_D, as α and R_c vary (see, for example, Thwaites 1960).

The most important moral to be drawn from all these considerations is that already noted at the end of Section I. 5.5, that there is no cessation of dependence on R when R reaches large values—marked variations in non-dimensional quantities being still prominent for R around 10^6. Before this was fully realized, much wind-tunnel work, in which models were tested at Reynolds numbers from 10^5 to 10^6 in the hope of getting information on full-scale flows at Reynolds numbers of about 10^7 or more, was practically useless.

Later, it became accepted that, since at the Reynolds numbers relevant in full-scale aeronautics (Section I. 5.3) almost the whole boundary layer is turbulent, the main aim in model testing should be to ensure this, by combining as high a Reynolds number as could conveniently be achieved with a sufficiently high level of tunnel turbulence or with suitable trip wires or roughness elements on the model (Pankhurst and Holder 1952). By these means the major features of the flow pattern can be correctly reproduced—although, to be sure, the detailed turbulent-boundary-layer characteristics are not identical, and certain features at high angles of incidence (see below), depending on the detailed state of the boundary layer very near the leading edge, are not reproduced well.

At a still later date, the possibility of large increases in the area of laminar flow being achieved, even at the high Reynolds numbers of full-scale flight, which would lead to very important reductions in C_D, began to be extensively studied (Goldstein 1948*a*). In contrast to the work just described, this requires the use of wind-tunnels of extremely low turbulence (Chapter X). The aerofoil must also be very smooth, and often is specially designed to have accelerated external flow over as large a fraction (say 0·5) of its surface as is compatible with other requirements. In addition, transition may be delayed by 'boundary-layer suction', boundary-layer fluid being sucked away through a suitable porous surface; this helps to stabilize the boundary layer by reducing R_δ, as well as by changing the distribution of vorticity to one of a more stable type, and the power required for such suction is much less than the power saving due to the reduction of C_D. Difficulties arise, however, because the tendency of any roughness elements (say, of height ϵ) to promote transition is increased by the reduction of δ and consequent increase of ϵ/δ; in addition, operational difficulties associated with the practical use of porous or specially smooth surfaces have so far prevented their adoption in aeronautics.

A more widespread form of 'boundary-layer control' uses a variety of devices to prevent local separations. These include the sucking away of the entire boundary layer at a 'slot', on the downstream shoulder of which a completely new boundary layer becomes attached. The aerofoil shape near the slot can be designed so that the external flow downstream of the slot is much slower than that upstream, and in this way a large retardation is achieved without separation (Goldstein 1948*a*). Alternatively, separation can be avoided by devices such as 'vortex generators', which are tiny vanes whose action increases the mixing in the turbulent boundary layer above its equilibrium level, and so promotes the transport of vorticity towards the wall.

As the angle of incidence α of an aerofoil is increased, the external flow velocity develops a higher and higher peak at the leading edge,

which depends on the fact that velocities in irrotational flow must be greatest on the inside of a bend, and builds up most rapidly if the leading-edge radius of curvature is low. Sooner or later, the retardation following this peak produces separation close to the leading edge, followed by an extensive wake region including the whole upper surface of the aerofoil; there is loss of lift, and a very large increase in drag, and the aerofoil is said to be stalled.

Before the stall is reached, there can be a local separation of a laminar layer at the leading edge, followed so closely by transition in the separated layer that reattachment is made possible; this 'short bubble' condition is dangerous, as further increase of α may lead with unpleasant suddenness to complete stalling (Owen and Klanfer 1955). On the other hand, at lower Reynolds numbers (but still greater than 10^6) one may find instead a 'long bubble' extending with increase of incidence to give a gradual, and therefore safer, stall. There are many other complications of stalling behaviour; these sometimes include oscillations of large amplitude in the separation position and wake shape; 'hysteresis' is also common, with the stall ceasing, as α is gradually decreased, at a lower value than that at which it appeared when α was increased (Farren 1935).

Three-dimensional wing aerodynamics will not be discussed here, as the general account of the thin-wake theory and of the varieties of possible surface topography in separated flow (Sections 2.2 and 2.7; note especially the discussion of 'tip stalling') are equally applicable when the boundary layer is wholly or partly turbulent.

On the other hand, we may note the useful comparison that has been made (Allen and Perkins 1951) between flow over slender bodies of revolution at high angle of incidence and the development in time of the flow around a circular cylinder which suddenly begins to move through a field. The basis of this comparison is that, as a large lump of fluid sails past the yawed body, it is confronted with an obstacle of circular cross-section whose position relative to the lump changes at the rate $U_\infty \sin\alpha$. This may cause the lump of fluid to develop a boundary layer of axial vorticity, growing as described in Section 2.1 and then separating, first at the rear and then farther forward, as described in Section 2.2. Next, the wake, left behind the 'cylinder' in its motion relative to the lump, grows to its steady size, becomes unstable and begins to cast off vorticity of alternating sign (Section 4.1). Interpreting this development in time as a development with distance along the body as the lump moves downstream from the nose, we are led to a

possible picture of the flow, Fig. II. 34, which experimental studies have confirmed. Such flow has the practical advantage of a substantial lift force centred reasonably far back from the nose, but may have the disadvantage of a fluctuating side force (normal to the plane in which the axis of the body is yawed), due to the first cast-off vortex leaving at some times from one side and at others from the other.

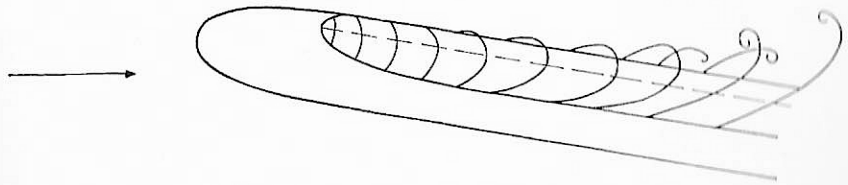

FIG. II. 34. Flow around a yawed body of revolution.

This very brief survey of a variety of complete flows in Section 4 has shown in part how knowledge of boundary layers can be used to illuminate whole flow patterns. To go farther, one must combine this knowledge with a study of the properties of possible external flows. This is the aim of the companion volume, *Incompressible Aerodynamics*.